

5

Volcanism

Burning mountains and volcanoes are only so many spiracles serving for the discharge of the subterranean fire ... And where there happens to be such a structure on conformation of the interior parts of the Earth, that the fire may pass freely and without impediment from the caverns therein, it assembles unto these spiracles, and then readily and easily gets out from time to time ...

Bernhard Varenius, 1672, quoted in Sigurdsson (1999), p. 148

5.1 Melting and magmatism

The German geographer Varenius (1622–1650) was one of the first to suggest that volcanic activity is ultimately caused by the escape of hot melted rock from the interior of our planet. Written at a time when most geologists believed that the Earth's interior is filled with molten rock, the source of the melt was not problematic: Any break or fracture would allow molten rock to leak out to the surface, just as puncturing the skin of an animal allows blood to flow out. However, with the study of solid earth tides and the advent of seismology at the end of the nineteenth century, it became plain that the bulk of the Earth is solid and the origin of magma became less obvious.

At the present time we believe that melted rock is a secondary manifestation of the thermal regime of our planet and that heat transport by magma is of slight importance compared to thermal conduction and lithospheric recycling, at least on the Earth. Volcanism and its subsurface accompaniment, igneous intrusion, is, nevertheless, an important process affecting the surface of the terrestrial planets, to the extent that almost no planetary surface seems to have escaped its effects.

Once-molten material from their interiors diversifies the surfaces of many, if not most, planets and satellites. Basalt has even erupted onto the surfaces of large asteroids such as Vesta, although this took place at a time when now-extinct heat-producing elements were active. In the outer Solar System the surfaces of icy satellites exhibit flows of congealed water-rich melts reflecting low-temperature “cryovolcanism.” Although the materials differ, the morphology of all these flows is similar, a manifestation of similar physical processes.

Table 5.1 *Heat budget of the Earth*

Source	Heat flow (10^{12} W)	Percent of total
Oceanic plate recycling, excluding crust formation	23.1	55
Intra-crustal radiogenic heat (mostly continental)	6.6	16
Conduction through continental plates	5.0	12
Oceanic crust formation ^a	3.1	7.4
Conduction through oceanic plates	2.9	6.9
Intra-continental advection (erosion, orogeny, magmatism)	1.1	2.6
Volcanic centers	0.2	0.5
Totals	42.	100.

Data from Sclater *et al.* (1980). Estimated accuracy of each entry ca. 10%.

^a Assumes oceanic crust is generated at $18 \text{ km}^3/\text{yr}$, which advects 1.81 MJ/kg .

5.1.1 Why is planetary volcanism so common?

One might suppose that volcanism acts as a kind of relief valve for pent-up heat in the interior of large Solar System bodies. Although there may be some truth to this idea (the planetary volcanic resurfacing event that affected Venus some 700 Myr ago is often supposed to mark an episode of high subsurface temperatures), a detailed inventory of the Earth's heat flow shows that volcanic heat transport accounts only for a small fraction of the total heat lost from our own planet's interior (Table 5.1), which is otherwise dominated by plate recycling (62% of the total) and lithospheric conduction (37%, including heat transported by oceanic crust formation). The amount of heat transported by volcanism, q_{vol} , can be estimated from the volume rate of eruption, Q_E , by:

$$q_{\text{vol}} = \rho(c_p\Delta T + \Delta H_f)Q_E \quad (5.1)$$

where ρ is the density of the magma brought to the surface, c_p its heat capacity, ΔT the temperature difference between the erupted magma and the surface, and ΔH_f is the enthalpy of fusion of the solid magma. The volume rate of eruption is often estimated from the volume of magma observed on the surface and the duration of an eruption, allowing estimates of the heat flux from volcanism alone. When compared to the heat flux conducted through the lithosphere, the volcanic flux is usually found to be small, except in the case of Io, whose heat transport does seem to be dominated by the eruption of magma (probably ultramafic silicate magma, accompanied by large amounts of the volatiles sulfur and SO_2). We do not have good estimates of the eruption rate on Venus during its short volcanic resurfacing event, but there, too, volcanic heat transport may have dominated its planetary heat flow. Venus should serve as a warning against too-simple classifications of planetary heat transfer: Different processes may dominate at different times in a planet's history.

Classifications are, nevertheless, useful, if one keeps their approximate nature in mind. A common and appealing classification of planetary heat transfer is the triangular ternary

diagram (Solomon and Head, 1982), borrowed from igneous petrology and illustrated in Figure 5.1a. Dividing planetary heat transfer into lithospheric conduction, plate recycling and volcanism, whose sum must equal 100%, one plots small bodies and one-plate planets close to the conduction vertex, the Earth near the plate-recycling vertex and volcanic bodies like Io close to the volcanic vertex. An alternative classification diagram is shown in Figure 5.1b in which heat transport is plotted versus mean mantle temperature, normalized by the melting temperature. On this one-dimensional diagram we also see the three processes, conduction, convection, and volcanism, but now laid out on a line reflecting the role of increasing internal heat generation. Volcanism, however, is not considered a unique mode of heat transport, but as an accessory phenomenon that can occur in any of the three regimes, although it becomes more important as the mean temperature rises.

The transition between pure conduction and convection occurs where the temperature of the mantle rises to about half its melting temperature, when viscous creep becomes important and the mantle's viscosity drops to about 10^{21} Pa-s. Because of the strong temperature dependence of solid-state creep, discussed in the last chapter, this regime tends to be self-regulating and can accommodate a large range of heat transport. However, once large-scale melting occurs the viscosity drops very rapidly to 10^3 Pa-s or even less, and the rate of heat transport, proportional to the inverse cube root of viscosity – see Equations (4.19) and (4.26) – increases million-fold. Heat transport rates higher than those sustained by such magma oceans are possible, but here we enter the realm of giant planet or even stellar interiors for which the concept of a planetary surface disappears, so we defer this topic to other texts.

Volcanism occurs on planets dominated by each of the major modes of heat transport. This is partly due to the physical nature of melts: no matter where they are produced, melts, once formed, are typically more mobile and less dense than their parent materials and so they may rise to the surface, leaving their parents behind. However, the principal reason for volcanism seems to be the highly variable susceptibility of planetary materials to melting. The ease with which materials melt varies with both position in the planet and composition of the material.

Melting in a convecting planet is most likely to occur just below the conductive thermal boundary layer. The boundary layer itself is, of course, the coldest part of the convecting system and temperatures rise linearly with increasing depth (refer back to Figure 4.1). This steep rise ends at the base of the thermal boundary layer where the temperature gradient becomes approximately adiabatic (Box 5.1). If the melting temperature were constant, melting would begin much deeper still, at the bottom of the convecting region. However, pressure increases the melting point, so the location where melting begins is established by a competition between the rate at which the temperature rises and the rate at which the melting point increases.

Clausius–Clapeyron equation. É. Clapeyron (1799–1864) in 1834 first deduced that the pressure derivative of the melting point of a substance is proportional to its latent heat of

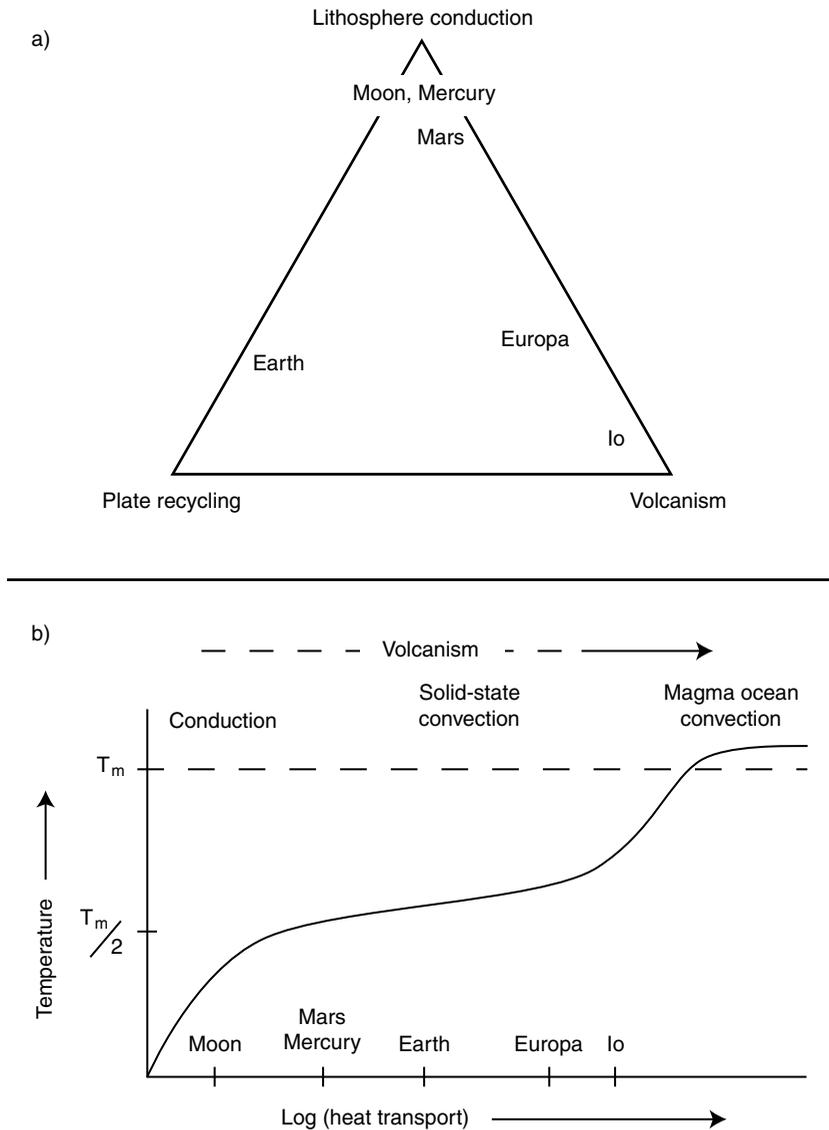


Figure 5.1 Mode of heat transport as a function of process. (a) Location of various planets and moons with respect to the three major heat transport processes of heat conduction through the lithosphere, plate recycling, and volcanism. (b) Dependence of mean mantle temperature and the transport process on net heat transport. As the amount of heat transport increases, the mode of transport switches from conduction to solid-state convection to liquid-state magma ocean convection. Surface volcanism may occur at any stage of this progression, although it is more likely to occur at net heat transport increases.

Box 5.1 The adiabatic gradient

The pressure experienced by materials in a planetary interior frequently changes as they move about. Because of the slow conduction of heat into large masses of material, this motion commonly takes place with little or no heat exchange to the surroundings. Nevertheless, compression or expansion of the material does change its internal energy and, therefore, its temperature varies as it ascends or descends. Such temperature changes are called *adiabatic* (equivalently, constant entropy or isentropic, as long as the process is also reversible). Adiabatic temperature changes play an important role in both convection and volcanism. The characteristic adiabatic gradient is a crucial concept in describing these processes.

The adiabatic gradient can be derived from fundamental thermodynamics in various ways. One of the simplest is to note that the entropy, S , is a state variable that is typically a function of only the pressure P and temperature T (in more special circumstances it may also depend on the composition, especially the latent heat during melting, the magnetic field, or other variables that affect the internal energy of the moving material), expressed as $S(P, T)$. Then standard multivariable calculus tells us that a change in the entropy can be expressed in terms of changes in temperature and pressure as:

$$dS = \frac{\partial S}{\partial T} dT + \frac{\partial S}{\partial P} dP. \quad (\text{B5.1.1})$$

Recall the definitions of the heat capacity at constant pressure, c_p , and volume thermal expansion coefficient α_v :

$$\begin{aligned} c_p &\equiv T \frac{\partial S}{\partial T} \\ \alpha_v &\equiv \frac{1}{V} \frac{\partial V}{\partial T} = \rho \frac{\partial V}{\partial T} \end{aligned} \quad (\text{B5.1.2})$$

where ρ is the density of the material. To these equations add the thermodynamic Maxwell relation between derivatives:

$$\frac{\partial S}{\partial P} = - \frac{\partial V}{\partial T}. \quad (\text{B5.1.3})$$

Then, inserting (B5.1.3) into (B5.1.1) and using the definitions (B5.1.2), we obtain an expression for the entropy change in terms of material properties:

$$dS = \frac{c_p}{T} dT - \frac{\alpha_v}{\rho} dP. \quad (\text{B5.1.4})$$

The adiabatic (reversible, no heat exchange) condition assures that $dS = 0$, so that the temperature changes with pressure according to:

$$\left. \frac{dT}{dP} \right|_{\text{adiabatic}} = \frac{\alpha_v T}{\rho c_p}. \quad (\text{B5.1.5})$$

Box 5.1 (cont.)

Finally, applying the hydrostatic relation between pressure and depth z and local gravitational acceleration g , $dP = \rho g dz$, we obtain the standard expression:

$$\left. \frac{dT}{dz} \right|_{\text{adiabatic}} = \frac{\alpha_V g T}{c_P}. \quad (\text{B5.1.6})$$

For the Earth's mantle, typical values of these constants are $\alpha_V = 3 \times 10^{-5} \text{ K}^{-1}$, $T = 1600 \text{ K}$, $c_P = 1000 \text{ J}/(\text{kg K})$ and $g = 10 \text{ m/s}^2$, resulting in a gradient of about 0.5 K/km . This is far smaller than the conductive temperature gradient near the Earth's surface, about 30 K/km . Nevertheless, across the entire 3000 km thickness of the Earth's mantle, if the gradient were independent of depth, then a temperature increase of about 1500 K would be implied, exclusive of the temperature jumps across the hot and cold conductive boundary layers at the bottom and top of the mantle. The adiabatic gradients in the other planets and satellites are smaller than that of the Earth, but the gradient, nevertheless, plays an important role in planetary-scale bodies, especially in relation to the gradient in the melting temperature of planetary materials.

melting. Stated in modern terms as the Clausius–Clapeyron equation, the pressure derivative of the melting temperature T_m is:

$$\frac{dT_m}{dP} = \frac{\Delta V_m}{\Delta S_m} \quad (5.2)$$

where $\Delta V_m = V_{\text{liq}} - V_{\text{solid}}$ is the volume change upon melting and $\Delta S_m = S_{\text{liq}} - S_{\text{solid}}$ is the entropy change upon melting, often expressed as the latent heat L divided by the melt temperature, $\Delta S_m = L/T_m$. The volume change upon melting is typically about 10% of the specific volume of a substance and ΔS_m is typically a few times the gas constant, based on Boltzmann's relation $S = R \ln W$, where R is the gas constant and W the probability of a given state (Pauling, 1988, p. 387). Table 5.2 lists the slope of the melting curve for several pure substances of geologic interest.

Decompression melting. Comparing the slopes of these melting curves with the adiabatic gradient, about 16 K/GPa for silicates, makes it clear that the adiabatic gradient is generally less steep than the melting curve of common minerals, at least at low pressures. We will see later that this must be modified at high pressures where mineral phase transformations take place, but at least near the surface of silicate planets it is clear that melting is most likely to occur just below the lithosphere, while at greater depths the planet may remain solid.

When hot, deep-seated solid material rises toward the surface by solid-state creep, its temperature gradually approaches the melting curve and, if the melting curve is reached, magma forms. This is one of the principal causes of melting in the Earth and probably the other silicate planets. It is called pressure-release or decompression melting. The other principal cause of melting, at least in the Earth, is the reduction of the melting point of silicates through the addition of volatiles, principally water. This is known as flux melting.

Table 5.2 Dependence of melting point upon temperature for various minerals

Mineral	Volume change upon melting, ΔV_m^a (cm ³ /mol)	Volume change as a fraction of molar volume, $\Delta V_m/V$	Entropy change upon melting, ΔS_m (J/mol-K)	Slope of melting curve at 1 bar, dT_m/dP (K/GPa)
Ice Ih (0 to 0.2075 GPa)	-1.634	-0.083	22.0	-74.3
Ice VI (0.6 to 2.2 GPa)	1.65	0.120	16.2	102.0
Quartz	1.96	0.086	5.53	355.0
Forsterite	3.4	0.072	70.0	48.0
Fayalite	4.6	0.094	60.9	75.0
Pyrope	8.9	0.077	162.0	55.0
Enstatite	5.3	0.157	41.1	128.0

Silicate data from Poirier (1991), water data from Eisenberg and Kauzmann (1969).

^a ΔV_m adjusted to agree with melting curve slope.

The peculiar melting behavior of water in icy bodies complicates this picture: Increasing pressure *decreases* the melting point of ice to a minimum of 251 K at a pressure of 0.208 GPa, after which the melting point increases again at an average rate of about 55 K/GPa. This permits the existence of stable subsurface liquid oceans in bodies such as Europa and possibly others in the outer Solar System, but makes it difficult for pure water to reach the surface.

Although the effect of pressure on the melting curve is of great importance in planetary interiors, the effect of composition, and of mixed compositions in particular, is probably even greater. It is not possible to understand volcanism on the Earth and other silicate planets without understanding the melting of heterogeneous mixtures of different minerals. Even on the icy satellites the melting behavior of mixtures of ices probably dominates their cryovolcanic behavior.

5.1.2 Melting real planets

Planetary composition: rocky planets. The composition of planetary bodies is ultimately determined by the mix of chemical elements that they inherited when they condensed from an interstellar cloud of gas and dust. Most of this material is too volatile to condense into rocky or icy planets: 98% of the mass of the Solar System is H and He, augmented by about 0.2% of “permanent” noble gases such as Ne and Ar. Of the remaining 1.8% of the mass, about 3/4 comprises “ices” and only 1/4 forms the high-temperature *rocky* material from which the terrestrial planets are built. Table 5.3 lists oxides of the major elements present in the “rocky” component of Solar System material. More than 90% of this rocky material is composed of only four elements: O, Fe, Si, and Mg.

The listing of elements as oxides in Table 5.3 is purely conventional: These elements are actually found in more or less complex minerals that are combinations of the simple

Table 5.3 *Cosmic abundances of metal oxides*

Metal in oxide combination	Abundance by mass (%)
FeO	38.6
SiO ₂	30.6
MgO	21.7
Al ₂ O ₃	2.2
CaO	2.1
Na ₂ O	1.9
All others	2.9

Data from Table VI.2 of Lewis (1995).

oxides. The four most abundant elements typically produce a mixture of the minerals olivine (Mg₂SiO₄ or Fe₂SiO₄) and pyroxene (MgSiO₃ or FeSiO₃) plus metallic Fe. Doubly charged iron and magnesium ions are rather similar in size and readily substitute for one another in the crystal lattices of olivine and pyroxene, which, thus, commonly occur as solid-solution mixtures of both elements. These minerals, along with their high-pressure equivalents, comprise the bulk of the Earth and other terrestrial planets, moons, and asteroids. Geologists are more familiar with rocks that contain a higher proportion of the less abundant elements Al, Ca, Na, and others. These elements generally form minerals of lower density than olivine and pyroxene and so have become concentrated in the surface crusts of differentiated planets.

Planetary composition: icy bodies. “Icy” materials, listed in Table 5.4, are more volatile than those forming the terrestrial planets and are, thus, mostly confined to the outer Solar System. The format in Table 5.4 is also conventional, listing the elements O, C, N, and S as chemical species that condense from a slowly cooling gas of average solar composition that is dominated by H. Water ice is by far the most abundant species, but carbon may occur as methane, as listed here, or as the more oxidized CO or CO₂. In comets, carbon seems to be present mainly as CO and CO₂ ices, often loosely bound in water as clathrates, as well as in more complex hydrocarbon “tars.” Nitrogen may occur as N₂ rather than as ammonia, and sulfur may form compounds with other elements.

The main lesson from this brief discussion of planetary composition is that all planets and satellites are heterogeneous mixtures of a variety of different chemical species. Although the proportions may vary depending upon their location in the Solar System and the chemical and physical accidents of their assembly, planets are anything but pure chemical species. This fact is the root cause of volcanic phenomena, and it requires a careful inquiry into the complex process of melting.

Melting rocks. Our most common experience with the melting of a solid is also one of the most misleading: Everyone is familiar with the conversion of solid ice into liquid water as heat is added. Probably everyone also knows that this takes place at a fixed temperature,

Table 5.4 *Cosmic abundances of ices*

Chemical species	Abundance by mass (%)
Water, H ₂ O (6.4% bound to silicates)	53.8
Methane, CH ₄	33.0
Ammonia, NH ₃	11.0
Sulfur, S	2.2

Data from Table VI.2 of Lewis (1995).

0°C at 1 bar, and that this temperature remains constant until all of the ice is converted into water. This behavior is typical of pure and nearly pure materials, such as fresh water. However, planetary materials are usually far from pure and so the melting behavior of heterogeneous mixtures of materials is most relevant in a planetary context.

Studies of the melting and reactions of complex mixtures of materials is as old as the “science” of alchemy, but a clear understanding of its basic principles only emerged in 1875 when Yale physicist J. W. Gibbs (1839–1903) published his masterwork “On the Equilibrium of Heterogeneous Substances.” Austerely written and published only in the *Transactions of the Connecticut Academy*, it took many years for the scientific community to absorb the principles that he set forth. In addition to mechanical work and internal energy, Gibbs associated energy, which he called the “chemical potential,” with each different chemical species and phase in a mixture of materials. Using the tendency of the entropy of an isolated system to increase, he defined the conditions under which reactions and phase changes occur in thermodynamic equilibrium and showed how to perform quantitative computations of the abundances of each species in a chemical system, once the chemical potential of each reactant is known. Much of the research in petrology and physical chemistry over the subsequent century has centered about measuring these chemical potentials (now known as the Gibbs’ free energy) of a wide variety of substances at different temperatures and pressures. The detailed application of these methods to the melting of ices and minerals is discussed in standard texts, such as that of McSween *et al.* (2003).

Melting of solid solutions. For a basic understanding of volcanic processes, it is enough to recognize that there are two fundamental types of melting in mixed systems. The first occurs in systems in which the different components dissolve in one another in both the liquid and the solid phase. Illustrated in Figure 5.2a for a mixture of iron and magnesium olivine at atmospheric pressure, the pure end member forsterite (Mg₂SiO₄) melts at a single temperature of 2163 K, while fayalite (Fe₂SiO₄) melts at the lower temperature of 1478 K. Mixtures of the two components, however, do not have a single melting temperature but melt over an interval that may be larger than 200 K, depending on the mixing ratio. The pair of curves connecting the pure endpoints on Figure 5.2a indicates this melting range. The lower curve, the solidus, marks the temperature at which the first melt appears at the given composition. The upper curve, the liquidus, marks the temperature at which the last solid

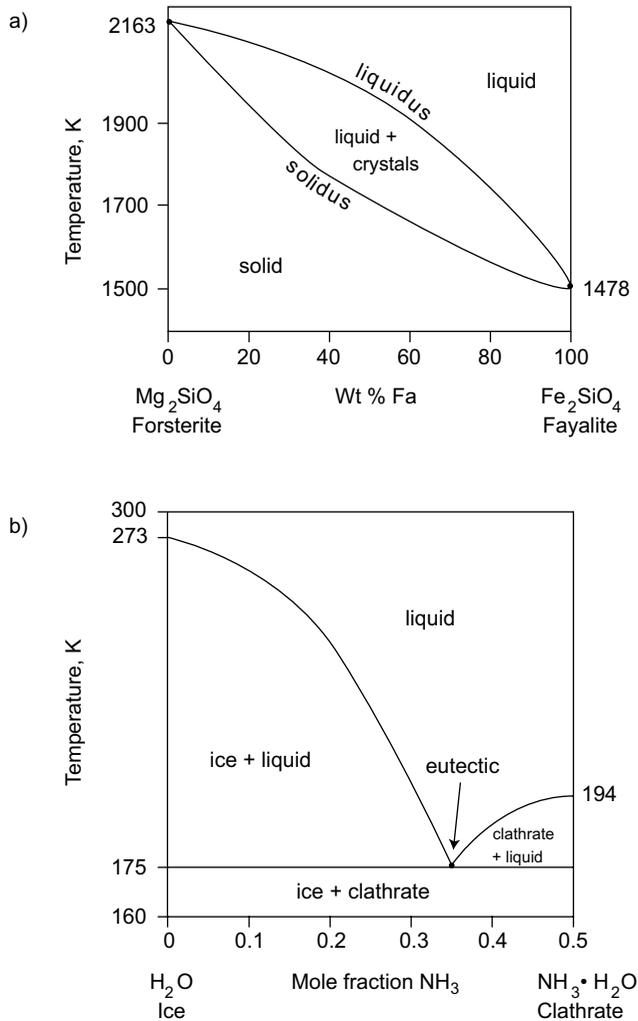


Figure 5.2 Melting relations in heterogeneous mixtures of substances. (a) Melting of a mixture of two materials that dissolve in one another, forming a solid solution. This example is for the pair of silicate minerals forsterite and fayalite. Note that melting of the solution occurs over a considerable interval of temperature. (b) Melting of a mixture of materials that do not form a solid solution but crystallize as distinct phases. This example is for water ice and water–ammonia clathrate, simplified after Figure 1 of Durham *et al.* (1993). Melting also takes place over a range of temperatures except at a single point, the eutectic.

crystal disappears. In between, a mixture of crystals and liquid is present. The crystals and melt do not, however, have the same composition: The crystals are always richer in magnesium (the higher melting point end member) than the melt. The equilibrium compositions of crystals and melt at any given temperature can be read off the diagram at the intersection

of a horizontal line drawn at the given temperature and initial composition on the plot with the liquidus and solidus lines.

Eutectic melts. The second type of melting behavior is illustrated in Figure 5.2b for a simplified version of the melting of a mixture of pure water and water–ammonia clathrate, $\text{NH}_3\text{-H}_2\text{O}$. Water and ammonia clathrate do not mix in arbitrary proportions, but form nearly pure compounds that separately melt at 273 K and 194 K, respectively. When crystals of the two species are mechanically mixed together, however, they react to form a liquid solution at about 175 K, less than the melting temperature of either pure end member. This first melt, called the eutectic composition, is composed of about 0.36 NH_3 by mole fraction. As the temperature continues to rise, what happens depends upon the mixture of crystals. The crystals always remain pure, but the melt composition changes as more crystals melt and mix into the liquid. If the overall composition is richer in ice than the eutectic melt, then all of the ammonia clathrate reacts with the water to form the liquid and only ice crystals are present in contact with the melt, whose composition is indicated by the line to the left of the eutectic point. As the temperature continues to rise, more and more of the water reacts with the melt until an upper temperature is reached at which all of the ice crystals disappear, also indicated by the line to the left of the eutectic point. If the original mixture of crystals is richer in ammonia clathrate than the eutectic composition, then all of the water crystals disappear at the eutectic temperature and a mixture of liquid plus ammonia clathrate crystals persists until the temperature reaches the line to the right of the eutectic point.

Complex melting. Real materials may exhibit either type of behavior in different ranges of composition due to partial solubility of one phase within another or more complex relations due to thermal decomposition of one phase before it finally melts. Despite the complexity of such behavior, it is all governed by Gibbs' rules and, with sufficient experimental data, the melting relations of any mixture of materials can be understood. The number of components that must be added to understand real rocks, however, is distressingly large. Ternary and quaternary diagrams have been devised to represent the mixtures of three or four components (Ehlers, 1987), but in the Earth as well as the other planets, many more than four elements, in addition to volatiles such as water and CO_2 , are present and the situation commonly exceeds the ability of any graphical method to illustrate the outcome. At the present time one of the frontiers in this field is gathering all of the data that has been collected by several generations of petrologists and physical chemists into computer programs that use Gibbs' thermodynamics and various models of mixing to predict the outcome of any natural melting event.

Pyrolite and basalt. A simple generalization, however, is possible for the terrestrial planets. As described above, most of their mass is composed of a mixture of olivine and pyroxene. Adding to this the "second tier" elements such as Al, Ca, Na, and K in the form of either feldspar (at low pressure) or garnet (at high pressure), geochemist A. E. Ringwood (1930–1993) concocted a hypothetical material he called "pyrolite" that forms a fair approximation of the bulk composition of any rocky body in our Solar System. When this material melts the first liquid appears at a eutectic temperature of about 1500 K and has a composition generally known as "basaltic." Basalt is a name applied to a suite of

dark-colored rocks rich in Fe, Mg, and Ca, among others, with about 50% of SiO₂. It is the typical rock produced on Earth at mid-ocean ridges, forms the dark mare of the Moon, and underlies extensive plains on Venus and Mars. Eucrite meteorites, believed to originate from the large asteroid Vesta, are basaltic in composition. Basalt is the quintessential volcanic melt from rocky bodies in the Solar System. Even on the Earth's continents, where more SiO₂-rich volcanic rocks are common, volcanologists have been known to describe volcanic activity as “basically basalt” because basalts from the Earth's mantle are now believed to provide most of the heat for even silica-rich volcanism.

Role of pressure in melting. Pressure affects the melting behavior of rock both by changing the properties (volume, entropy) of a given mineral phase and by changing the stable phases of the minerals themselves. As olivine is compressed it undergoes a series of transformations to denser phases, assuming the structure of the mineral spinel beginning at about 15 GPa (depending on composition and temperature; there are actually two spinel-like phases), then transforming to a still denser perovskite phase at 23 GPa. These phase changes are clearly seen seismically as wave velocity jumps in the Earth's interior. The phase changes are reflected in the melting curve, as shown in Figure 5.3a, which illustrates the behavior of the solidus and liquidus of the olivine–pyroxene rock known as peridotite (equivalent to basalt-depleted pyrolite, and taken to represent the Earth's mantle) as a function of pressure up to 25 GPa (equivalent to that at a depth of 700 km in the Earth or the core-mantle boundary in Mars). It is clear that the steep melting gradients computed for individual minerals in Table 5.2 cannot be extrapolated to great depths, although the average melting temperature does continue to rise as pressure increases. Figure 5.3b expands the low-pressure region to show several adiabats along with the solidus and liquidus. Note the low slope of the adiabats in comparison with the solidus, as well as the change in slope of the adiabats when melt is present. A hot plume rising along one of the adiabats begins to melt when the adiabat intersects the solidus and continues melting as it rises further, although in reality the melt separates from the solid when more than a few percent of liquid is present, causing a compositional change in the residual material that must be modeled in more detail than is possible from Figure 5.3b.

Flux melting. The properties of silicate magmas are strongly controlled by small quantities of volatile species, particularly water, which has a high affinity for the silica molecule. The dramatic effect of water in lowering the melting point of rock of basaltic composition is illustrated in Figure 5.4, where water saturation is seen to lower the melting point by as much as 500 K at a pressure of a few gigapascals. This strong dependence of melting temperature on water content leads to the possibility of melting caused by addition of volatiles – flux melting. The name comes from the practice of adding “fluxes” like limestone to iron smelters to produce a low melting point slag. On Earth, fluxing by water is particularly important in subduction zones, where hydrated minerals formed in the oceanic crust sink into the mantle. As these minerals heat up, they lose much of their water, which then invades the overlying crustal wedge and lowers the melting point of these rocks. The result is the massive volcanism associated with the overriding plate in subduction zones. As a measure of the importance of water fluxing, note that the average eruption temperature

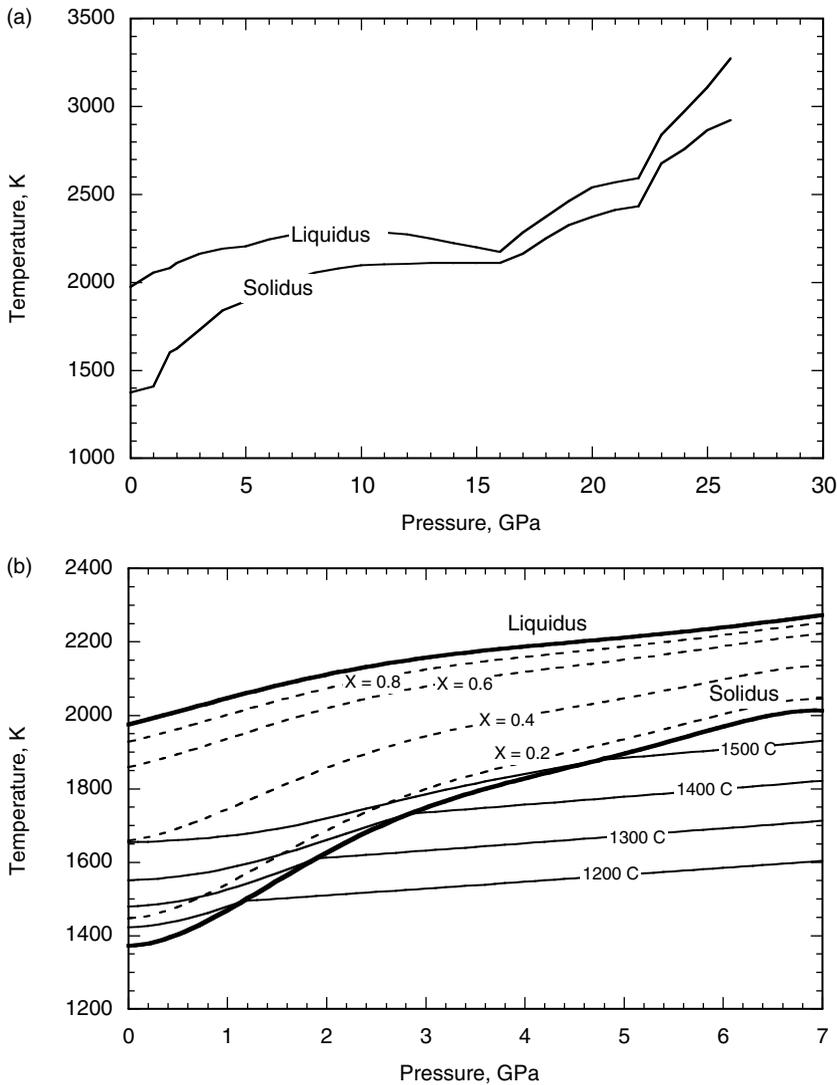


Figure 5.3 Phase diagram of peridotite representative of the Earth's mantle. (a) The solidus and liquidus temperatures of peridotite to a pressure of 25 GPa. The inflections in these curves are due to phase transformations of the constituent minerals as the pressure is increased. After Ito and Takahashi (1987). (b) Detail of the peridotite phase curve (heavy solid lines) to 7 GPa showing adiabats for various temperatures (light solid lines; temperatures indicated in centigrade to facilitate comparison with petrologic data) and light dashed lines showing different degrees of partial melting. Data from Ito and Takahashi (1987), computational method after McKenzie and Bickle (1988).

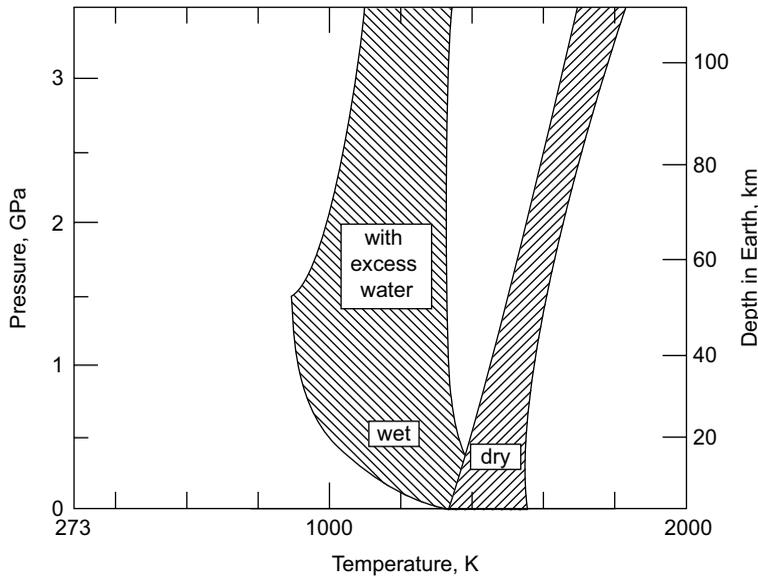


Figure 5.4 The effect of water on the melting temperature for magma of gabbro composition. The shaded regions indicate the interval between the solidus and liquidus. Note that the gabbro–eclogite transition takes place just below the solidus temperature of dry gabbro. The presence of excess water in the magma dramatically lowers the melting temperature at high pressure, by as much as 500 K for pressures near 1 GPa. After Figure 6–12 of Wyllie (1971).

of silica-rich island arc magmas is only about 1200 K, whereas the eruption temperature of basaltic lava is typically about 1500 K. Because silica-rich rocks are more susceptible to the fluxing effects of water than silica-poor rocks, the overall effect of flux melting in subduction zones is to enhance the abundance of silica in melts produced in this environment. The high-silica granitic rocks of Earth's continents may thus be a direct consequence of subduction plus water. It is presently unknown whether this mechanism also plays a role on planets that lack plate recycling, but this makes the discovery of silica-rich granitic rocks on other terrestrial planets a question of great interest. To date, there is no clear evidence for such rocks on Mars, in spite of a brief flurry of excitement over the possible discovery of an andesitic composition rock by the Pathfinder mission – since retracted by the discovery team.

Carbon dioxide also plays a large role in magmas as its presence reduces the solubility of water – water and CO_2 are the dominant gases released in volcanic eruptions. On the Moon, where water is scarce and the lunar mantle is more reducing, CO seems to have been the major gas released during eruptions of basaltic magma. The important role of these volatiles in driving explosive volcanic eruptions will be discussed below in more detail.

Cryovolcanism. Cryovolcanism on the icy satellites presents a still-unsolved problem. We do not yet have samples of the material that flowed out on their surfaces, so the

exact composition of the cold “lavas” on these bodies is still conjectural, except that spectral reflectance studies reveal an abundance of water ice. But pure water has a relatively high melting temperature for these cold worlds and, moreover, it is denser than the icy crusts through which these “cryomagmas” apparently ascend, making it difficult to understand how pure liquid water could reach the surface. So either the crusts are mixed with some denser phase (silicate dust or maybe CO₂ ice), or the liquid water is impure, mixed perhaps with ammonia or bubbles of some more volatile phase that lower its average density.

5.1.3 Physical properties of magma

The mechanics of volcanic eruptions and flows are largely dependent upon the physical properties of magma as it separates from its source rock, rises from depth, and spills out onto a planetary surface. Eruptions and flows generally occur so rapidly that chemical equilibrium is not attained and so it is physics, not equilibrium chemistry, which governs the final stages of magma evolution. The most important property in eruptions is the viscosity of the melt, which is a strong function of temperature, composition, pressure, and crystal content.

The viscosity of silicate magmas depends strongly upon their silica content. The small tetravalent silicon ion bonds strongly with four oxygen ions to form very stable tetrahedra. In silica-poor minerals, such as olivine, the tetrahedra are isolated and their charge is balanced by adjacent metal ions. However, as the silica content increases the tetrahedra share corners, forming linear chains in pyroxenes, then sheets and ultimately create a space-filling lattice in pure SiO₂. Silica tetrahedra can, thus, form long polymers in silica-rich melts and, similar to the polymers in carbon-based compounds, the viscosity increases rapidly as the length and abundance of the polymer chains increase. At the same temperature, granitic melts with SiO₂ abundances in the range of 65–70% typically have viscosities about 10⁵ times larger than basaltic melts with SiO₂ near 50%. Moreover, as temperature increases and breaks up the polymers, the viscosity of silica-rich melts changes much faster than that of basaltic melt. These relations are shown in Figure 5.5.

Water and silicate magma. The tendency of silica tetrahedra to polymerize also explains the strong dependence of the viscosity of silica-rich magmas on water content. Water does not dissolve in a silicate melt as the triatomic molecule H₂O. Instead, one of its hydrogen atoms bonds with an oxygen ion in the melt to form a pair of OH⁻ radicals that bond with the silica tetrahedra. In the process, as shown in Figure 5.6, silica polymers are broken into shorter pieces and the viscosity consequently drops. This effect is important only in very silica-rich melts: The viscosity of basaltic melts is hardly affected by dissolved water, as shown in Table 5.5, which compares the viscosity of wet and dry silica magmas at typical terrestrial eruption temperatures. Thus, water both lowers the melting temperature of silica-rich melts, such as granites, and decreases their viscosity. Granitic melts, thus, typically arrive at the surface with high water contents and low temperatures, whereas basaltic magmas are hot and relatively dry. This circumstance has major implications for the processes

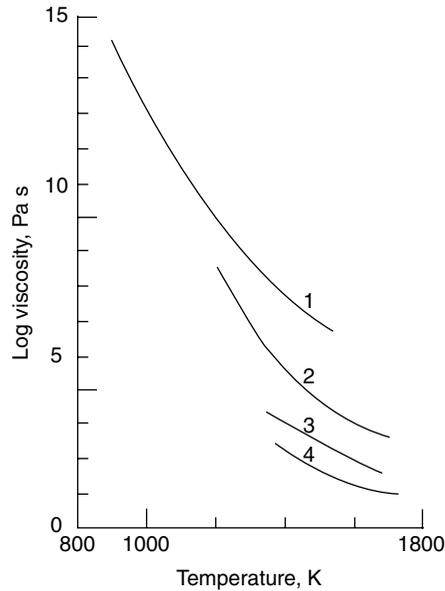


Figure 5.5 The viscosity of silicate melts depends strongly upon both temperature and silica content. The four curves are shown for dry but increasingly silica-poor rocks: (1) rhyolite, (2) andesite, (3) tholeiitic basalt, (4) alkali basalt. After Figure 2–4 of Williams and McBirney (1979).

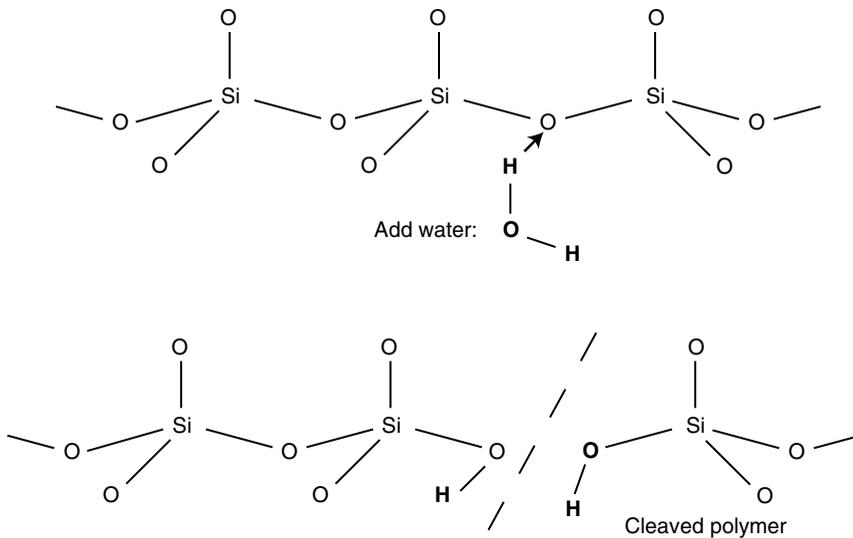


Figure 5.6 Water has a strong affinity for silica polymers. When a water molecule reacts with a long silica polymer chain in the upper half of this figure, it easily breaks the polymer into pieces, while inserting OH groups into the resulting silicate chains. Simple counting of O–H and Si–O bonds shows the same number before and after the insertion, so this process is almost energy-neutral. Breakdown of the silica polymers lowers the viscosity of silicate magma.

Table 5.5 Effects of water on the viscosities of silicate melts

Melt composition	Approximate SiO ₂ content (Wt %)	Temperature (K)	Viscosity dry (Pa s)	Viscosity with dissolved H ₂ O (Pa s)
Granite	72	1058	10 ¹¹	10 ⁴ (5% H ₂ O)
Andesite	60	1423	10 ³	10 ^{2.5} (4% H ₂ O)
Tholeiitic basalt	50	1423	10 ^{2.2}	10 ² (4% H ₂ O)
Olivine basalt	48	1523	10 ¹	10 ¹ (4% H ₂ O)

Data from Williams and McBirney (1979).

that occur in an eruption and lend silica-rich magmas a dangerous tendency to explode due to exsolution of their water.

Viscosity and crystal content. Magmas are typically not entirely liquid. Upon eruption, most magmas contain a heterogeneous assemblage of liquid, crystals, and bubbles of gas. The presence of both crystals and bubbles strongly affects the viscosity and flow properties of the mixture. If the magma contains more than about 55% by volume of solids it may not be able to flow at all: The solid crystals interlock with one another and the flow of the bulk magma is controlled by solid-state creep of the crystal framework rather than the liquid matrix. For crystal contents ϕ up to about 30% by volume, the Einstein–Roscoe formula gives the average viscosity of the liquid mass η in terms of the viscosity η_0 of the liquid alone (McBirney and Murase, 1984):

$$\eta = \frac{\eta_0}{(1 - \phi)^{2.5}}. \quad (5.3)$$

The viscosity of natural magmas varies with crystal content even more than this equation suggests, because the crystals that form in a cooling magma are typically less rich in silica than the magma itself. Thus, as crystallization proceeds the melt becomes progressively enriched in silica and, because of polymerization, the viscosity rises dramatically. Because of its importance in terrestrial volcanology, the rheology of silicate melts has received a great deal of attention. Unfortunately, the same cannot yet be said of the water-rich melts present in the icy satellites of the outer Solar System, for which only a few rheological measurements exist.

Bingham rheology. In addition to increasing the viscosity of the melt, the presence of a dense mass of crystals alters the flow properties of magma still more profoundly. In 1919 the chemist E. C. Bingham (1878–1945) discovered the peculiar behavior of a dense emulsion of solids while trying to measure the viscosity of paint (Bingham and Green, 1919). Paint, like magma, is a dispersion of small solid particles in a liquid, although in the case of paint it is usually compounded from a ceramic powder like titanium oxide mixed into organic oil. Bingham was trying to measure its viscosity by forcing paint under

pressure through narrow capillary tubes and using a well-established equation for the flow of a viscous fluid through a tube to determine its viscosity. Much to his surprise, he discovered that the paint would not flow at all until the pressure reached some finite threshold, after which the rate of flow depended linearly on the pressure, as he had expected. Bingham quickly realized that he had made an important discovery and could, for the first time, explain why wet paint does not immediately flow off a vertical wall: Paint has a finite yield stress, now called the “Bingham yield stress,” that must be exceeded before it can flow. The thickness of a layer of fresh paint is proportional to this yield strength, and does not depend on the viscosity. Previous to Bingham’s work, viscosity alone was used to determine the quality of paint until the American Society for Testing Materials compared 240 samples of paint at its Arlington, VA, laboratory. In this test many samples, prepared to have the same viscosity but, unbeknownst to the testing staff, having different yield stresses, ran off the boards of a fence and left gaping, unsightly, bare spots. Following his success in explaining this fiasco, Bingham went on to a distinguished career during which he coined the term “rheology,” introduced the “poise” as a unit of viscosity, and founded the Society of Rheology.

Although it might seem that the rheology of paint has little in common with volcanic phenomena, it has been abundantly shown that lava is also a Bingham material and that the Bingham yield stress is a crucial parameter for computing the length and thickness of lava flows and domes. Indeed, almost any dense mixture of solid and liquid is likely to behave as a Bingham material: Even kitchen staples such as mashed potatoes (surely you have noticed that mashed potatoes can only be piled so high, after which the pile collapses – their Bingham yield stress has been exceeded!), apple sauce, and pudding are properly described as Bingham materials, as are basaltic magma, mudflows, and rock glaciers. Although the Bingham yield stress is thus a central parameter in many applications, it unfortunately cannot be computed from first principles for nearly any mixture. There are literally hundreds of empirical equations relating the Bingham yield stress to solid volume fraction, particle shape, size and liquid composition, but the ability of these formulas to predict the yield stress of previously unmeasured materials is practically nil. The reason for this failure is that the Bingham stress depends on the surface energy of contact between the solids in the mixture. This surface energy depends on so many presently unknown factors that prediction is nearly impossible: All current work is empirical.

The relation between shear strain rate and shear stress for a Bingham material is given by:

$$\begin{aligned} \dot{\epsilon} &= 0 && \text{for } \sigma < Y_B \\ \dot{\epsilon} &= (\sigma - Y_B) / \eta_B && \text{for } \sigma \geq Y_B \end{aligned} \quad (5.4)$$

where Y_B is the Bingham yield stress and η_B is the Bingham viscosity. This equation will be used below to describe the behavior of lava flows on a planetary surface. First, however, we need to understand how magma gets up to the surface of a planet in the first place.

5.1.4 Segregation and ascent of magma

When solid material from deep within a planetary body begins to melt, small pockets of melt first form at high-energy locations such as grain boundary intersections and where different crystals can react to produce eutectic liquids. At first, these tiny melt pockets have no tendency to join together and remain trapped in the rock. At this stage an often-overlooked phenomenon controls the fate of these small particles of melt. If the surface contact energies of the melt and crystals surrounding them permits the melt to wet the crystal faces and run along the grain boundaries, melt will begin to accumulate into larger volumes. On the other hand, if the contact angle between the melt and the solid crystals is greater than about 60° , the melt beads up and much larger volumes of melt must form before the melt can separate from its parental rock (Watson, 1982). In both silicate rocks and water–ammonia mixtures the contact angle is small and melt readily percolates out of the matrix. However, some combinations of materials, such as liquid iron and silicate, have larger contact angles and percolation is strongly inhibited.

Magma percolation flow. In silicate rocks, when the melt fraction exceeds a few percent, the melt begins to percolate along grain boundaries and flows out of the source rock. The process of “Rayleigh distillation” then controls the chemical evolution of the melt, in which the continuously extracted melt carries away the elements that enter the liquid and, thus, the composition of the source material gradually changes. The contrasting process of “batch melting” occurs when the melt remains in chemical communication with the parent rock.

If the matrix through which the melt percolates can be treated as a rigid structure, the flow of the melt is described by the Darcy equation (which was originally devised to describe the percolation of water through porous rock: See Section 10.2.2). In one dimension, this equation relates the volume discharge of fluid (magma in this case) per unit area Q to the gradient of pressure driving the flow and the viscosity η of the liquid,

$$Q = -\frac{k}{\eta} \frac{dP}{dz}. \quad (5.5)$$

The permeability k has dimensions of (length)² and depends upon the size and spacing of the pores through which the magma percolates (see Turcotte and Schubert, 2002 for more on permeability and how to calculate it). The most uncertain part of this equation is the permeability, but this equation has, nevertheless, often been used to estimate the length of time necessary to, say, differentiate a basaltic crust on a heated asteroid or to produce enough magma to feed an observed surface flow. In this case the vertical pressure gradient is equal to the difference in density between the liquid and solid matrix times the gravitational acceleration, $dP/dz \approx \Delta\rho g$. Taking the permeability very roughly to equal the square of the grain size d , the timescale for magma to flow out of a layer of thickness h is given by:

$$t_{\text{percolate}} = \frac{\phi \eta h}{d^2 \Delta\rho g}. \quad (5.6)$$

For an asteroid like Vesta, the magma percolation time is only about 60 yr for a 125 km thick mantle (half of Vesta's radius), assuming a density difference of 300 kg/m^3 , a grain size of 1 mm, total melt fraction of 10%, and a basaltic magma viscosity of $10 \text{ Pa}\cdot\text{s}$. This timescale is very short compared to the thermal heating timescale, and indicates that the rate-determining step in Vesta crust formation is not melt percolation but the rate at which its mantle heats up. This seems to be the case in many circumstances: In general, melt percolation is so fast that melt leaves its parental rock as fast as it is formed.

Diapirs vs. dikes. Studies of depleted source rocks on the Earth suggest that the simple rigid percolation model is quite inadequate. It appears that melt in hot rocks, especially if they are deforming, quickly collects into pockets and veins that are much larger than the grain size. These melt rivulets join to form larger veins that drain the mass of source rock more efficiently than uniform percolation. As the magma accumulates in ever larger bodies, the difference in density between the melt and matrix becomes more important and buoyant bodies of melt may begin to slowly rise through the high-viscosity source rock. Many book illustrations depict magma, especially highly viscous silica-rich magma, in this stage as rising in mushroom-shaped diapirs, similar to those depicted in Figure 4.9. However, petrologists are currently in doubt about the validity of this picture.

A low-density fluid, such as magma, enclosed in a higher density but deformable matrix, has two means of ascending through the matrix. One is a diapir, discussed above. The other is a dike, a vertical fluid-filled crack that pierces directly through the matrix and permits much more rapid ascent of the fluid. Whereas diapirs exploit the viscous property of a fluid, developing when a low-density fluid displaces an overlying higher density viscous fluid, dikes exploit the elastic property of the enclosing material. Hot rocks, however, exhibit both viscosity and elasticity, depending on the timescale: They are best described as Maxwell solids, as described in Section 3.4.3. Whether the rise of magma is governed by the viscous or elastic response of the surrounding rocks depends on timescale, and, thus, on the ratio between the viscosity of the magma and that of the host rocks. The precise conditions for the dominance of one process or the other are still somewhat uncertain: It is presently an area of active research (Rubin, 1993). However, near the surface it seems clear that most basaltic magmas ascend via dikes. This is also true for at least some granitic magmas (Petford, 1996), so the following discussion focuses on the mechanics of dike ascent. An older, and now-discredited model of volcanic eruption is discussed in Box 5.2. Whereas this "standpipe" model has some apparent successes, in the light of the discussion below it cannot possibly be correct, but it is still of interest because the elastic dike model cannot, as yet, reproduce the major success of the old, impossible model!

Dikes differ from simple cracks for two major reasons: They are filled with a viscous liquid and, because of gravity, the pressure that the fluid exerts on the walls of the vertical crack differs greatly between its top and bottom. Much of our present understanding of dikes rests on the summer research of material scientist Johannes Weertman. Weertman, who has made fundamental contributions to the study of dislocations and creep in solids, is also a highly regarded glaciologist. He may have become interested in dikes while watching a stream flowing over the surface of a glacier disappear into a crevasse and wondered

Box 5.2 The standpipe model of magma ascent

A striking observation made by pilots flying along the volcanic range of the Andes or the Aleutian volcanic chain is that the summits of all the volcanoes seem to be at nearly the same elevation (Ben-Avraham and Nur, 1980). This holds even though the bases of the volcanic constructs often differ greatly in elevation: Extruded lavas build their ultimate cone up to an apparently fixed elevation. A good planetary example of the same relation is the summit elevations of the four major volcanic centers on Mars. The summit calderas of the three major volcanoes on the Tharsis Rise – Arsia Mons, Pavonis Mons, and Ascraeus Mons – all rise to an elevation of almost 20 km above the Martian datum, each about 12 km above their bases near the summit of the Tharsis Rise (Table B5.2.1). Olympus Mons, however, rising from the lowlands of Amazonis Planitia far to the west of the Tharsis Rise, *also* rises to about 20 km, even though its base lies 1 km below the Martian datum.

The accordance of these summits was stunningly discovered near the beginning of the Mariner 9 orbital mission. Arriving at Mars during the height of a planetary dust storm in 1972, the first images showed only a uniform haze of red dust. However, as the dust began to settle, four dark spots – the tops of the major volcanoes – began to emerge almost simultaneously. Planetary geologist Hal Masursky, seeing these spots, immediately proposed that they were the summits of giant volcanoes, much to the astonishment of the planetary geologic community. Their simultaneous appearance out of the haze was an indication of the similarity of their summit elevations.

Even though the concordances of height of most volcanoes are approximate, their consistency does not seem accidental. This concordance has been “explained” for many years by a model that might be called the “standpipe” model, because it posits that the magma rises up a rigid open channel (pipe) and settles at the level of hydrostatic equilibrium.

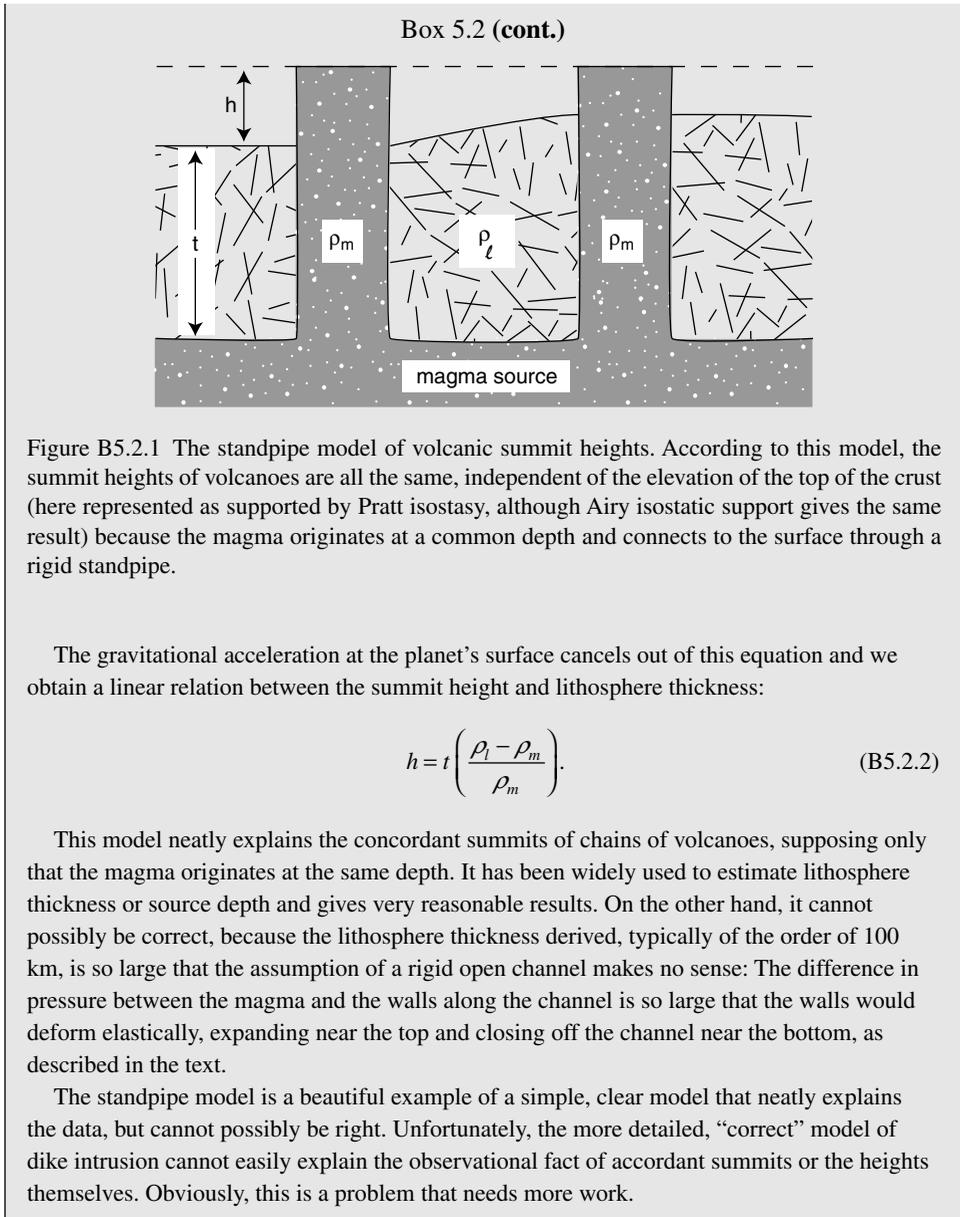
Illustrated in Figure B5.2.1, the model supposes that the magma rises from its source depth through a rigid lithosphere of density ρ_l . The pressure in the magma, of density ρ_m , is equal to the pressure of the lithosphere in the magma source region at the base of the lithosphere. Because the magma is less dense than the lithosphere, the column of magma must be taller than the thickness of the lithosphere, of thickness t , by an amount h , equal to the height of the volcano’s summit above the planetary datum, independent of the actual height of the volcano’s base. Balancing pressures,

$$(t + h) \rho_m g = t \rho_l g. \quad (\text{B5.2.1})$$

Table B5.2.1 *Elevations of the major Martian volcanoes*

Volcano	Edifice height (km)	Base elevation (km)	Summit elevation (km)
Olympus Mons	22	–1	21.229
Ascraeus Mons	15	3	18.225
Pavonis Mons	10	4	14.058
Arsia Mons	12	6	17.761

Data from USGS (2003).



whether the stream would ever be able to fill the crevasse. These ruminations led to a fundamental paper (Weertman, 1971) that elucidated the role of gravity and elasticity of the wall rock in determining the shape of a vertical dike (from a mechanical point of view, a dike is just a water-filled crevasse turned upside-down). One of his most important discoveries is that dikes cannot be arbitrarily deep: They are strictly limited in their vertical extent by the

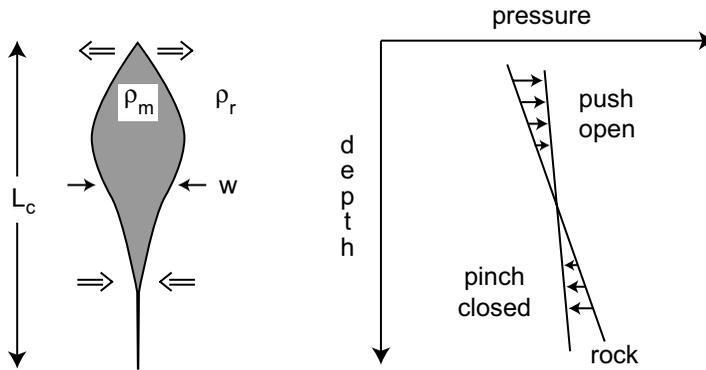


Figure 5.7 Pressure as a function of depth in a vertical dike. Because the magma in the dike is less dense than the surrounding rock, the pressure in the dike falls less rapidly (here shown in highly exaggerated form as a vertical line in the right half of the figure). If the average pressure in the dike and the surrounding rock are equal, the pressure in the dike exceeds that of the enclosing rock at the top of the dike, whereas the pressure in the rock exceeds that in the dike at its bottom. The magma thus pushes the crack open at its head, while it is squeezed closed at its tail, forcing its way upward through the rock. The actual length of the crack L_c is a function of the elastic properties of the surrounding rock as well as the pressure drop in the crack and is computed in the text.

elastic deformation of the surrounding matrix. This fact implies that the quantity of magma that can rise in a dike is quantized into a fixed volume.

Dike mechanics. The full analysis of the length and ascent velocity of a fluid-filled crack is complex (Rubin, 1995), but some simple order-of-magnitude estimates can illustrate the main outlines of the theory. As magma rises into a vertical, slowly moving crack, the low density of the magma compared to the wall rock means that the pressure in the crack falls less rapidly than in the surrounding denser rock (Figure 5.7). If the magma and rock are at the same pressure in the source region, the pressure at the head of the crack will, thus, exceed that in the adjacent rock and the top of the crack will tend to balloon outward. This extra stress at the crack tip, if large enough, may rip apart the rock ahead of the crack and permit the mass of magma to ascend. However, as the tip of the crack balloons, the tail of the crack grows narrower because of the elastic reaction of the surrounding medium (this is similar to the bulge that forms adjacent to a loaded area on an elastic half space – or the bulge next to a person who sits down on a springy sofa). As the crack lengthens the tail nearly pinches off, although the fluid in the crack prevents it from closing completely. At this stage the rising crack can accept no more magma and it continues to ascend toward the surface as an independent pod of hot magma.

A simple relation between the length L and width w of such a crack is obtained by equating the average stress generated by the crack in the elastic medium to the pressure drop between the head and the tail of the crack. The elastic stress is computed from the strain, $\varepsilon = w/L$, times Young's modulus E : $\sigma = Ew/L$, according to the definition (3.9). The pressure drop through the crack is just $(\rho_r - \rho_m)gL = \Delta\rho gL$. Equating these stresses, we obtain a

relation between the critical crack length and width that is nearly identical to the relation derived from the detailed theory of crack-tip dynamics (Rubin, 1995):

$$L_c = \sqrt{\frac{E w}{\Delta\rho g}}. \quad (5.7)$$

For parameters appropriate for the Earth, this tells us that a 1 m wide vertical dike would have a height of about 2 km, in reasonably good accord with geologic observations. This result, however, does not give us an independent way of estimating the crack width and length. Weertman solved this difficulty by balancing the elastic stress of the crack against a regional extensional stress T , which he considered necessary to permit the crack to ascend. Although dikes do generally ascend perpendicular to regional extensional stress, experiments on the injection of dyed liquids into gelatin matrices suggest that extension is not an essential factor in dike ascent. What has been neglected so far is the flow of the fluid included in the dike. Magma-filled dikes ascend at rates limited by the viscosity of the fluid and the width of the dike. A magma-filled dike cannot ascend so fast that the pressure drop in the viscous magma exceeds the pressure gradient in a static crack (otherwise the pressure gradient would reverse and the magma would decelerate), so the pressure drop due to the fluid flow provides another equation to determine w in terms of the rate at which magma flows in the dike. Using the definition of viscosity, Equation (3.12), it is easy to show that the mean velocity \bar{v} of a viscous fluid flowing through a channel of width w is, up to factors of order 2, given by:

$$\bar{v} \approx \frac{w^2}{2\eta} \frac{dP}{dz} = \frac{w^2}{2\eta} \Delta\rho g. \quad (5.8)$$

The volume discharge of a planar dike Q_d per unit length is equal to $\bar{v}w$. Solving for w in terms of the discharge, and inserting it into Equation (5.7), one can show that the length of a dike carrying a fixed discharge of magma Q_d is given by:

$$L_c = \frac{E^{1/2} (2Q_d \eta)^{1/6}}{(\Delta\rho g)^{2/3}}. \quad (5.9)$$

The most notable feature of this equation is its dependence on $1/g$. This has the surprising and important implication that the volume of a magma “quantum” ascending from a magma source, which is roughly equal to $L_c^2 w$, actually *increases* as the gravitational acceleration decreases. This makes a good deal of sense: In order to break through to the surface of a small body, the magma’s buoyancy force must overcome the resistance of the elastic medium through which it ascends. On a low-gravity body this means that the volume of magma must increase. On Earth these magma quanta are relatively small, a few 100 m³, and may account for the almost regular pulsing activity seen in erupting volcanoes: Each pulse represents the arrival of a new package of magma traveling up a dike connecting the surface with the magma reservoir below.

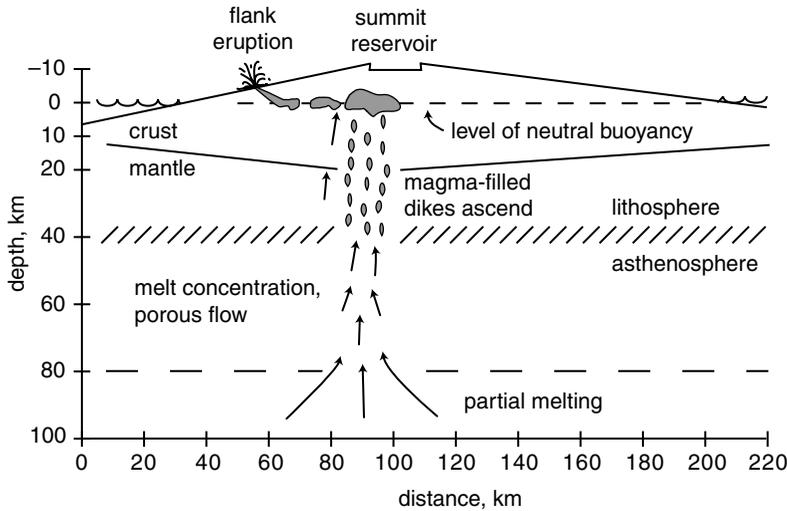


Figure 5.8 Ascent and eruption of magma beneath the Hawaiian volcanoes. Magma originates in the hot mantle below the volcanoes, concentrates into pods and pockets, and finally ascends to the surface in dikes. As it reaches the level of neutral buoyancy it stalls, collecting in magma chambers and moving laterally to emerge in flank eruptions. Summit eruptions occur when the driving pressure from new material becomes high enough to push magma from the level of neutral buoyancy up to the summit of the edifice. Figure simplified after Tilling and Dvorak (1993).

Eruption volume and gravity. This analysis shows that volcanic eruptions should become both more voluminous and more rare as the size of the body decreases. Lunar volcanic eruptions should be much larger and more catastrophic than terrestrial eruptions, a deduction that seems to agree well with the large volume of lunar lava flows. Going to still smaller bodies, many of the small icy satellites seem to have been volcanically resurfaced only once in their history, by an eruption so large that it covered nearly their entire surface.

Level of neutral buoyancy. The behavior of magma near the surface depends largely upon the density contrast between the magma and the surrounding rocks. Although the height to which magma can ascend depends upon the driving pressure at depth, this factor often seems to be eclipsed by the level at which magma achieves neutral buoyancy: That is, where the density of the magma equals that of the surrounding rock. First expressed by G. K. Gilbert in his famous monograph on the Geology of the Henry Mountains (Gilbert, 1880), this concept has found abundant support from detailed studies of the Hawaiian volcanoes (Ryan, 1987). Magma beneath Kilauea caldera rises until it encounters rocks of similar density, then spreads out laterally beneath the surface in the form of vertical dikes (Figure 5.8). The depth to the upper portion of these dikes fluctuates as the magmatic pressure fluctuates. When this pressure becomes especially high the top of the dike reaches the surface and magma pours out in a fissure eruption.

As magma-filled dikes approach the surface dissolved volatiles may come out of solution and form a pocket of gas that leads the liquid toward the surface, as discussed in more

detail in the next section. When this occurs the average density of the fluid filling the dike decreases and it may be possible for the dike to rise higher than the buoyancy of the liquid magma itself might suggest. Interactions between the liquid, gas and surrounding solid rocks then become complex and their consequences have yet to be fully understood.

Intrusion vs. extrusion. Magma reaching its level of neutral buoyancy has no further tendency to ascend and may become “stalled” underground, creating magma chambers and reservoirs. It may also spread out in the form of either vertical dikes or horizontal sills, depending on whether the local minimum principal stress is horizontal (dikes) or vertical (sills). When sills extend to a critical size that is controlled by the elastic properties of the overlying rock, they may bodily lift the overlying rocks and create a turtle-shaped intrusive mass named a “laccolith” by Gilbert. Laccoliths on Earth may reach several kilometers in diameter and uplift the overlying rocks by up to 1 km.

An important statistic for volcanism on any planet is the ratio between the volume of magma extruded on the surface and that intruded below the surface. Estimates for the Earth suggest that far more is injected below ground than ever reaches the surface, perhaps by as much as a factor of 40. The oceanic crust typically consists of about 0.5 km of extrusive pillow basalts that overlie a total of about 5–10 km of vertical dikes and plutonic gabbro (the intrusive equivalent of basalt), giving a ratio of intrusion to extrusion of 10:1 to 20:1. In continental rifts, basaltic lava has more difficulty reaching the surface through the low-density continental crust and this ratio may be still larger: A large fraction of the magma of the well-studied Central Atlantic Magmatic Province that formed as Africa rifted away from North America appears to be intrusive.

5.2 Mechanics of eruption and volcanic constructs

5.2.1 Central versus fissure eruptions

A common observation is that volcanic materials on the surface of a planet may either pile up in a heap, recognized as a volcanic center or mountain, or they may spread over a broad, low-lying area. In the latter case the source of the volcanic flow is often obscure, but when it can be located it frequently turns out to be a long fissure from which lava poured over a relatively short interval to feed the surface flows. Because such feeder fissures tend to cover themselves, they can be difficult to find without detailed topographic maps supported by high-resolution images.

What determines the pattern of central vs. plains volcanism is unclear: Every planet appears to possess both volcanic mountains and extensive volcanic plains, although the proportion of central to fissure eruptions varies greatly from one planet to another, or even from one location to another on a single planet. On Earth, we recognize volcanic centers that create steep-sided volcanoes such as Japan’s Mount Fuji, and low domes such as the islands of Hawaii. Earth also possesses broad volcanic plains such as the US’s Columbia Plateau or India’s Deccan Plateau. Venus similarly exhibits large central volcanoes, such as Sif Mons, that contrast with the broad volcanic plains that underlie most of the planet’s surface. Even the Moon, which seems to lack steep-sided volcanic mountains in favor of broad

mare basalt plains, possesses a volcanic center on the Aristarchus plateau. Recent images of Mercury from the MESSENGER spacecraft revealed a volcanic center southwest of the Caloris Basin, which contrasts with the otherwise planet-wide volcanic plains.

Mantle plumes and hot spots. Regional concentrations in the intensity of volcanic activity are often related to the activity of hot, buoyant plumes that rise through the planet's mantle (see Figure 4.9), carrying heat from depth as part of the normal convective heat engine that cools the planet's interior (Ernst and Buchan, 2003). As a new teardrop-shaped plume head nears the surface and its pressure drops, its temperature may cross the solidus. The melts that, thus, form quickly separate and rise further, either intruding the crustal rocks just below the surface or erupting onto the surface. Plumes eventually spread out in the mantle beneath the crust, generating melts at a lower rate than the initial spurt. Hot mantle material may continue to rise for a long time along the warm trail (the "plume tail") left in the wake of the original plume head. This extended flow of hot material becomes the source of a long-lived volcanic center. Earth's Hawaiian island chain is believed to originate as the Pacific plate drifts over such a long-lived source of magma rising from deep in the mantle. The Tharsis Rise on Mars may similarly be located over a long-lived plume in the Martian mantle. In the case of Mars, however, there are no moving tectonic plates and the large volume of Tharsis is attributed to the long-term accumulation of volcanic melts at one location. The evolution of Venusian coronae is likewise linked to the activity of plumes rising from its deeper mantle (Squyres *et al.*, 1992).

Although plumes can explain regional concentrations of volcanic activity, they do not determine whether the eruption will be either of the central or fissure type: On Earth, plume sources are invoked both for volcanic centers such as Hawaii or Yellowstone and for plateau basalts such as the Deccan or Siberian flows. Does magma composition play a role in determining whether activity is centralized or diffused into regional fissure systems? What about the persistence of the heat source – do long-lived sources of magma (plume tails) favor central activity, while short, hot pulses (plume heads) favor fissure-fed plains? These questions are presently unresolved.

The Earth is unique among the terrestrial planets in its possession of plate tectonics. Subduction-zone magmas are highly enriched in silica as well as volatiles from subducted oceanic plates bearing sediments and hydrated minerals. Subduction zones also tend to persist for geologic periods. The result is long, linear chains of central volcanoes such as the Andes or Aleutians. Hot, plume-generated, basaltic magmas may also intrude the base of silica-rich continental crust, melting the overlying rocks and creating local pockets of silica-rich melts that underlie volcanic centers such as Yellowstone, which are not related to subduction zones.

5.2.2 Physics of quiescent versus explosive eruptions

Volcanic eruptions can, in principle, be simple outpourings of liquid magma onto the surface of a planet. In practice, however, they usually involve a complex mixture of solid, liquid, and gas components whose behavior upon reaching the surface is anything but simple. One of the most consistent observations of terrestrial volcanic eruptions is that

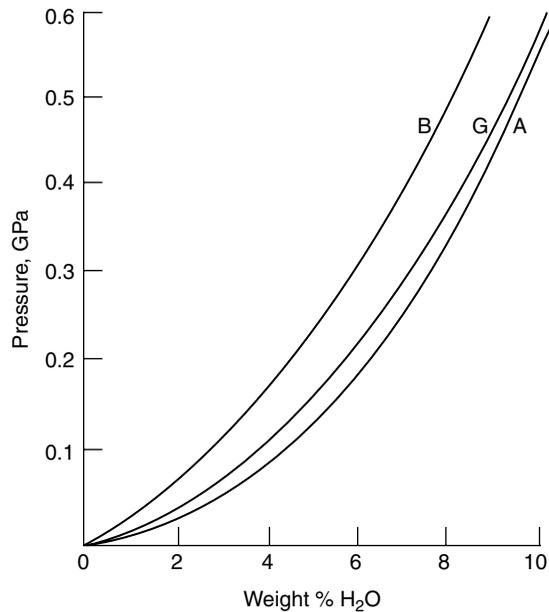


Figure 5.9 The solubility of water in magmas of different composition at a common temperature of 1373 K: B is basalt, G granite, and A is andesite magma. Decreasing the pressure greatly decreases the solubility for all compositions. Although all three materials can dissolve similar amounts of water at a given temperature and pressure, the eruption temperature of these three kinds of magma varies greatly on Earth. After Figure 2–13 in Williams and McBirney (1979).

they progress from gas-rich initial phases into the eruption of successively gas-depleted magmas, although the course of any one eruption may involve a complex alternation of gas-rich to gas-depleted pulses (Williams and McBirney, 1979). This progression is readily explained by the separation of gas from liquid magma as it rises toward the surface: The upper tip of rising dikes or the near-surface zones of masses of magma become enriched in gas that is vented as the dike or magma column breaches the surface. Gas-depleted liquid magma (often mixed with crystals) then follows.

The tendency for dissolved gases to separate from their parent magmas near the surface is a simple consequence of the pressure and temperature dependence of gas solubility. Gas solubility in a liquid generally increases with increasing pressure. This is especially true for water in silicate melts because of the strong affinity of water for silica. Measurements of the solubility of water in magma as a function of pressure, Figure 5.9, show that deep in planetary crusts silica-rich magmas may hold up to 10% water by weight, but at surface pressures this drops by almost two orders of magnitude. This tendency for depressurized liquids to exsolve gas is familiar to anyone who has quickly opened a sealed container of a carbonated drink: Upon opening, the pressure suddenly drops and bubbles of carbon dioxide appear throughout the liquid.

The consequences of gas exsolution near the surface depend strongly upon the viscosity of the magma and the rate at which the pressure drops. Fluid magmas, such as basalt, tend to erupt relatively quietly. Their viscosities are low (Figure 5.5) so that bubbles of exsolved water or carbon dioxide readily escape the magma, collecting in large pockets of gas at the tip of rising dikes. The presence of such gas pockets in moving dikes contributes to the seismically observed “harmonic tremor” that often precedes Hawaiian eruptions. When such a dike breaches the surface, the first material to erupt is mostly gas, driving the dramatic (but localized) fire-fountain activity that ushers in the main flow of magma onto the surface. Fire-fountaining may be renewed during a prolonged eruption as new dikes arrive to discharge their own gas pockets, then add their magma to the overall flow. Basaltic eruptions on the sea floor may not possess a gas-rich phase because the pressure beneath 4 km of seawater (about 0.04 GPa) is too large for much gas to exsolve. Such deep-sea eruptions are much more quiescent than eruptions onto the Earth’s surface. Venus’ surface pressure may likewise be large enough to suppress intense exsolution of volatiles and, thus, preclude explosive eruptive activity (presuming, of course, that Venus’ interior possesses Earth-like quantities of water or carbon dioxide).

Silica-rich magmas, such as andesites or rhyolites, have such high viscosities that volatiles have great difficulty separating from them. As pressures drop in rising magmas of this type, the volatiles form bubbles that remain trapped in the viscous melt. This fact, along with the strong pressure dependence of solubility, leads to a dangerous tendency for silica-rich volcanoes to catastrophically “explode.” Note that, although the word “explosion” is commonly used to describe catastrophic volcanic eruptions, these events are not actually explosions in the sense that a rapid conversion of solid to gas results in a sudden increase of pressure: In volcanic eruptions the pressure always *decreases*. This behavior strongly differentiates volcanic eruptions from impacts, in which large pressure increases do occur. The shocked minerals that characterize impacts have never been reliably associated with volcanic eruptions. The presence of such minerals, thus, serves to discriminate the two types of event.

Catastrophic, silica-rich eruptions can proceed from either fissures or central volcanoes, as demonstrated by deposits in Earth’s geologic record. However, no fissure eruptions have been observed during recorded history, so the following discussion will focus mainly on the eruptions of central volcanoes.

Silica-rich magmas are seldom observed reaching the surface directly. Instead, they accumulate for some time beneath the surface, cooling by conduction and interaction with surrounding groundwater and thus partially crystallizing as they lose their initial heat. Fluid pressure in the magma increases as more of the melt solidifies into crystals because fluids are excluded from the regular crystal lattice. Eventually this fluid pressure is released, either as a gas-rich eruption or in response to some unrelated event, such as the landslide that preceded the 1980 eruption of Mount St. Helens and suddenly uncapped its magma chamber. A sudden pressure release, from whatever cause, initiates a rapid chain reaction that we recognize as an explosive eruption.

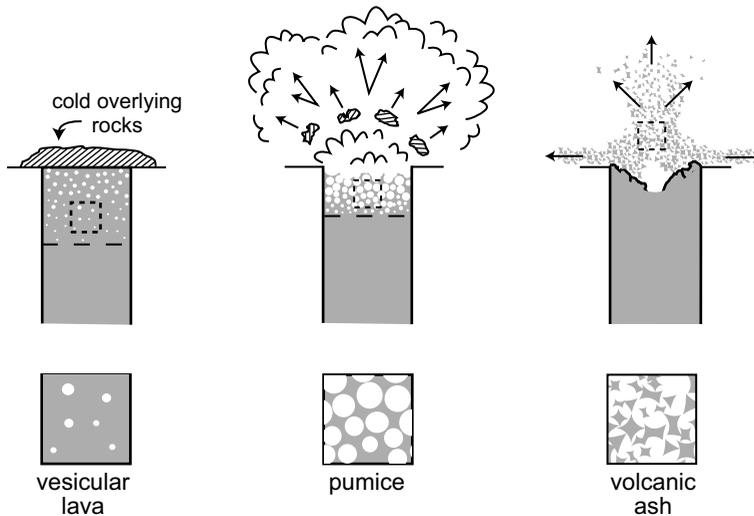


Figure 5.10 The upper row illustrates the sequence of events that occurs during an explosive volcanic eruption. At the beginning, pressure builds up below a strong cap sealing the volcanic vent. Bubbles exsolve from the magma as it cools, which create vesicular lava when it erupts on the surface (lower row). In the middle panel, the increasing pressure removes the cap overlying the vent and the sudden pressure release causes more gas to exsolve. The gases expand explosively, accelerating volcanic debris and magma to high speed. Frothy magma erupted at this stage is called pumice. In the right panel, so much material has been removed from the vent that it collapses, sealing in the magma below. The expanding gases disrupt frothy magma into small glass shards that mix with varying amounts of ambient air and produce volcanic “ash.”

Any sudden pressure release causes vapor to exsolve from the liquid magma. In a highly viscous, silica-rich magma the bubbles formed by this vapor cannot easily escape from the magma. Near the surface, where pressure is low, the bubbles grow large and the volume of the magma suddenly increases by a large amount. This bubbly froth spills out of the magma chamber onto the surface, continuing to expand as the pressure drops. It expands upward as well as outward and may accelerate to velocities of hundreds of meters per second. The magma may be completely dispersed by this large expansion, forming an emulsion of gas and magma fragments that is commonly called “volcanic ash,” even though no actual combustion takes place. The vapor cools rapidly as it expands, chilling the magma fragments, which often form tiny glass shards whose shapes are recognizably portions of the walls of former liquid bubbles. In more fluid magmas the bubble walls may have time to reform into spherical liquid droplets, as is observed for the silica-poor glassy products of lunar fire fountains.

The ultimate fate of such erupting gas/liquid emulsions depends strongly upon the ratio of gas to liquid (glass). Gas-poor magmas erupt as bubbly liquids in which the bubbles are widely separated from one another (see Figure 5.10, lower row). These magmas chill to

form lavas containing small, often roughly spherical cavities known as vesicles. This material is thus called vesicular lava. Even lunar basalts contain vesicles whose gas phase is now believed to have been carbon monoxide, CO. Magmas containing more gas cool to form a rock whose bubbles are nearly in contact, giving it an average density that may be less than that of water. Lavas of this type are called pumice. Volcanic ash results when the bubbles coalesce and the emulsion's volume is dominated by gas.

Gas-rich emulsions may expand at high speed. The ultimate velocity of such an expanding mixture is determined by the thermodynamic properties of the gas, in particular by its molecular weight and initial temperature. The expanding emulsion often incorporates other material from the vent walls, clots of gas-depleted magma or even cold rocks. These accidental inclusions are accelerated with the gas and may be thrown substantial distances from the vent. Such fragments are called volcanic bombs and pose a major hazard to volcanologists trying to approach the site of an active eruption. The impact of large volcanic bombs sometimes forms craters a few to ten meters in diameter many kilometers from the vent. Although volcanic debris may be thus accelerated to high speed, it is unlikely to exceed escape velocity of even moon-sized bodies. Box 5.3 explains how the maximum ejection speed is determined. Note that the size of the volcano itself is not a factor in determining the ejection speed – only the eruption temperature and nature of the gas are important.

As a gas-rich emulsion of hot gas and melt fragments expands above the surface it may reach substantial heights before falling back. Its initial velocity at the surface, v_{ej} , gives the maximum height that this mixture can reach ballistically. Equating its kinetic and gravitational potential energies, this height is given by $v_{ej}^2 / 2g$, where g is the surface acceleration of gravity (Figure 5.11a). On an airless body the mixture of gas and fragments may rise to considerable heights – the Prometheus plume on Io rises about 75 km above its surface – then spreads laterally, driven by the entrained gas, into a wide umbrella that rains back onto the surface over a broad area (Figure 5.11b).

When an atmosphere is present, the erupting emulsion may incorporate some of the surrounding atmosphere. The average density of this mixture may become lower than that of the ambient atmosphere as the incorporated gas is heated. In this case the erupted material rises still further as a buoyant plume (Figure 5.11c). On the Earth, such buoyant eruption columns commonly rise into the stratosphere, tens of kilometers above the surface. The incorporated glassy particles then drift with the local winds and rain out later, at a rate depending on their size. Fine volcanic ash may, thus, spread globally over the Earth, although most of the coarser volcanic ash falls closer to the vent. Many terrestrial volcanic ash deposits can be recognized thousands of kilometers from their sources.

Even when an eruption plume does not become buoyant, it spreads rapidly away from the vent. The emulsion of gas and glassy particles is then denser than the surrounding atmosphere, but the mass is still fluidized by the gas phase, much as a dry snow avalanche is fluidized by air incorporated with the snow particles. It, thus, spreads as a density current, often overrunning topographic obstacles near the vent. Such hot, mobile density currents are known as pyroclastic flows. They can be devastating to human life and buildings

Box 5.3 A speed limit for volcanic ejecta

When magma rises to the surface and dissolved gases come out of solution, the hot, high-pressure gases expand and lower the pressure. As the gas expands it accelerates both itself and any entrained solid or liquid droplets to high velocity. However, thermodynamics imposes a strict limit on the maximum velocity to which this material can expand. This maximum is mainly a function of the initial temperature and composition of the gas phase.

The gas itself attains the highest velocity: Any burden of entrained material lowers the ultimate velocity of the mixture. We thus focus on computing the maximum expansion velocity of the gas alone, with the understanding that any admixture of solid or liquid material slows the final velocity in proportion to the square root of its additional mass loading. We assume that, for the time period under consideration, the flow is approximately steady, with a reservoir of hot, high-pressure gas at pressure P_1 expanding through some complex but energy-conserving process to a final pressure P_2 .

Referring to Figure B5.3.1, consider two successive times during the steady expansion, t_A and t_B . At time t_A there is a mass m of gas on the left with a total energy equal to the sum of its specific internal energy e_1 and kinetic energy $1/2 u_1^2$ per unit mass times m :

$$m \left(e_1 + \frac{1}{2} u_1^2 \right) + (\text{energy of hatched region}) .$$

At time t_B the same mass of gas has emerged

on the right (this is the steady-flow approximation) and the total energy is now given by:

$$m \left(e_2 + \frac{1}{2} u_2^2 \right) + (\text{energy of hatched region}) .$$

Furthermore, in steady flow the energy in the

hatched region has not changed. Between the times t_A and t_B , the work done by the pressure P_1 on the mass on the left is $P_1 \Delta V_1$, where the volume change $\Delta V_1 = m/\rho_1$, where ρ_1 is the density

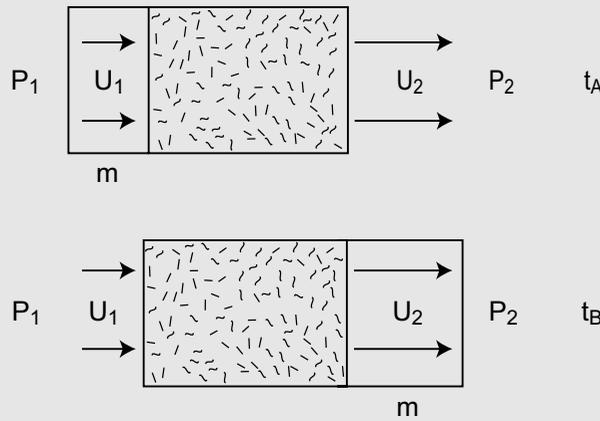


Figure B5.3.1 Schematic illustration of volcanic gases expanding steadily through a complex vent, represented by a hatched block. So long as the expansion does not add or subtract energy, the details of the expansion do not matter. The high-pressure gas on the left at time t_A expands so that its increase in kinetic energy per unit mass at t_B is equal to its decrease in enthalpy per unit mass, as described in the text.

Box 5.3 (cont.)

of the fluid on the left. Similarly, the work done by P_2 on the right is $P_2\Delta V_2 = mP_2/\rho_2$. Equating the sum of the energy and the work done at t_A and t_B then gives:

$$m\left(e_1 + \frac{1}{2}u_1^2\right) + m\frac{P_1}{\rho_1} = m\left(e_2 + \frac{1}{2}u_2^2\right) + m\frac{P_2}{\rho_2} \quad (\text{B5.3.1})$$

where the energy of the hatched region cancels out, because it does not change from t_A to t_B : This is the crucial assumption that no energy is added or lost during the expansion. We can cancel the common factor m and note that the definition of the specific enthalpy h is:

$$h \equiv e + \frac{P}{\rho} \quad (\text{B5.3.2})$$

so Equation (B5.3.1) becomes:

$$h_1 + \frac{1}{2}u_1^2 = h_2 + \frac{1}{2}u_2^2 \quad (\text{B5.3.3})$$

or, collecting like terms:

$$u_2^2 - u_1^2 = 2(h_1 - h_2). \quad (\text{B5.3.4})$$

If the initial velocity u_1 is either zero or much smaller than u_2 , as is usually the case in a volcanic eruption, we can neglect it and set u_2 equal to the maximum expansion velocity u_{\max} , which from Equation (B5.3.4) we find:

$$u_{\max} = \sqrt{2(h_1 - h_2)}. \quad (\text{B5.3.5})$$

For a perfect gas at temperature T the specific enthalpy is:

$$h = c_p T \quad (\text{B5.3.6})$$

where c_p is the specific heat at constant pressure (SI units are J/kg-K) and T is the temperature in K. Note that, although the molar heat capacity for many substances is similar, the heat capacity per unit mass depends strongly on the molecular weight of the material, so that low-molecular-weight gases typically have a much higher specific heat than high-molecular-weight gases and consequently expand faster. Hydrogen-powered volcanoes thus eject material much faster than volcanoes erupting water vapor or CO_2 .

If h_2 is much less than h_1 because of the strong cooling during adiabatic expansion, then we can write simply:

$$u_{\max} \approx \sqrt{2c_p T_{\text{magma}}} \quad (\text{B5.3.7})$$

where T_{magma} is the pre-eruption temperature of the magmatic gases. This equation provides a convenient and easily evaluated estimate of the maximum expansion velocity possible in volcanic eruptions. It gives a good estimate of the maximum observed velocity of volcanic bombs from terrestrial volcanoes. Some typical results are given in Table B5.3.1.

Box 5.3 (cont.)

Table B5.3.1 *Maximum expansion velocity in volcanic eruptions, Equation (B5.3.7)*

Working gas	Heat capacity, c_p (kJ/kg-K)	Magmatic temperature (K)	u_{\max} (km/s)
H ₂ O	2.0	1473	2.4
CO	1.02	1473	1.7
CO ₂	0.84	1473	1.6
H ₂	14.3	1473	6.5

It is possible to incorporate modifications of this simple formula for the presence of solids or liquids loading the gas, but there are no simple formulas because the results are sensitive to the details of how heat is exchanged between the gases and solid. As a start, one notes that the solids or liquids make only a negligible contribution to the pressure. Defining $s = m_{\text{solids}}/m_{\text{gas}}$, we can write for the density $\rho = (1+s)\rho_{\text{gas}}$, so using the perfect gas law the enthalpy of the gas itself is given by:

$$h_{\text{gas}} = \left(c_p - \frac{s}{1+s} R \right) T \quad (\text{B5.3.8})$$

where R is the gas constant. Values of s greater than zero clearly lower the enthalpy of the gas, but this neglects heat transfer between the entrained solids and liquids and gas during expansion. Further treatment requires modeling beyond the level of this book.

tens to hundreds of kilometers from a volcanic vent. The phenomenology of such flows is both complex and of great interest from many points of view. For more information the reader is referred to the recent monograph of Branney and Kokelaar (2002).

The ultimate deposits of explosive volcanic eruptions range from welded tuffs, which are deposited from density currents that are so hot that the glass particles weld together once they come to rest, to airfall tuffs in which the chilled, glassy magma particles fall relatively gently to the surface through either air or water. Less is known of deposits on airless bodies such as the moon. There, the chilled droplets of magma must be emplaced ballistically, with less ability to flow far from their original vent. An important characteristic of all such deposits is that they tend to blanket pre-existing terrain and, unlike water-laid sediments, may be deposited with initial slopes that follow the terrain rather than lying in initially horizontal beds.

Back at the vent from which the emulsion of gas and liquid magma erupted, changes occur as more and more material is ejected. The pressure on the deeper-lying magma is relieved as material from the top of the magma chamber is erupted (Figure 5.10). Volatiles dissolved in this deeper-seated magma then exsolve, creating more bubbles and increasing

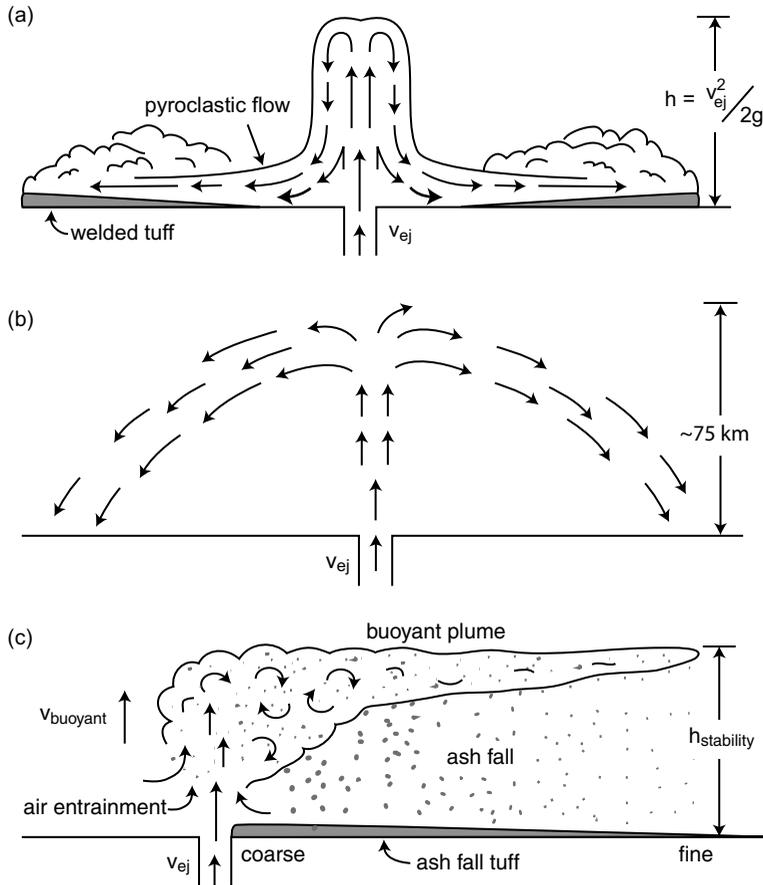


Figure 5.11 Panel (a) illustrates the ejection of an emulsion of magma and volcanic gas from a vent at high speed. The plume rises ballistically to a height h determined by the conversion of its kinetic energy to gravitational energy and then falls back. As it descends, it forms a hot density current known as a pyroclastic flow. When this material finally vents its gas and settles into a deposit on the surface it creates an ignimbrite or welded tuff. In Panel (b) the eruption occurs on an airless body. In this case the plume rises so high above the surface that it cools (by thermal radiation) before it descends to the surface. It spreads out as it rises, forming an umbrella-shaped plume such as those on Io. Panel (c) illustrates an eruption on a body with a dense atmosphere, such as the Earth or Venus. In this case the plume incorporates atmospheric gases and becomes buoyant, rising until its density equals that of the surrounding atmosphere at $h_{stability}$, after which it drifts laterally, responding to local winds. As it drifts, cooled volcanic ash falls out of the cloud and is deposited as loose volcanic tuff on the surface. The largest particles fall out first, the finer material later, producing a deposit in which the particle size grades laterally from coarse near the vent to fine farther away.

the magma's volume. This material then follows the first-erupted material out of the vent, further expanding and accelerating as it reaches surface pressures. This initiates a chain reaction in which progressively deeper material expands and flows out onto the surface at progressively higher velocities. This chain reaction ceases only when rock surrounding the magma chamber loses its lateral support and collapses into the void left by the magma that has now erupted onto the surface. Overlying rocks, if not initially removed by the violence of the eruption, also subside to fill the void. The final result is a depression, a volcanic caldera, surrounded and perhaps partially buried by the magma that has so recently left its original location. The size of the depression reflects the size of the original magma chamber and its included volume of unstable magma. The vents producing small eruptions, such as that of the 1980 eruption of Mount St. Helens, may not totally collapse because the surrounding rock is strong enough to support the evacuated cavity. Much larger magma bodies, however, leave caldera depressions that reach dimensions of hundreds of kilometers. Such collapse calderas are observed on most volcanically active bodies, including Venus, Mars, and Io as well as the Earth.

5.2.3 Volcanic surface features

Although nearly every volcanic eruption involves gas and liquid phases, the relative contributions of these two major phases vary widely from one eruption to another. At one extreme, some eruptions are driven almost entirely by gas, in which little or no magma may appear at the surface. At the other extreme, enormous volumes of liquid magma pour rapidly onto the surface with little or no accompanying gas. The morphology of the final deposits depends strongly upon the relative volumes of gas and liquid.

Maar craters. The structures most likely to be confused with impact craters are produced by gas-dominated eruptions. Eruptive vents are often nearly circular, are surrounded by a raised rim of ejecta, and are depressed below the pre-eruption surface, similar to impact craters. Such vents are called maar craters or tuff rings. On Earth, they frequently contain lakes (hence the name maar, which derives from the German word for a small lake). They form as volcanically heated gases breach the surface and eject a gas-fluidized mass of rock debris that frequently contains no magma. The gas may either be deep-seated, rising from depths of a few hundred kilometers in the case of diamond-bearing kimberlite pipes, or near-surface water that is explosively vaporized by contact with hot, rising magma. In either case the gas/debris expulsion velocity may be very high, several hundred meters per second, and the vent is often surrounded by a bedded deposit containing debris from great depth displaying bedforms that indicate high-velocity radial outflows of gravity currents initiated by the eruption. The volume of this ejecta (the tuff ring surrounding the vent) is often much smaller than the volume of the crater itself, indicating withdrawal or subsidence of the magma following the eruptive phase. Craters of this type on Earth include many examples in the Franconian Lake District, Germany, MacDougal and Sykes craters, among others, in the Pinacate Mountains of Sonora, Mexico, and Ubehebe crater in California's Death Valley. The latter crater is often described as a phreatic explosion crater because the

source of the water in this case appears to be near-surface groundwater. Maar craters are typically only a few kilometers in diameter.

It is difficult to recognize maar-type volcanic craters on other planets, largely because of their close resemblance to impact craters. In this case one often must appeal to the departure of volcanic vents from perfect circularity, their tendency to form linear clusters over subsurface dikes, and their small-volume rim deposits compared to impact craters. However, in some cases there is no ambiguity because gas-rich eruptions have been caught in the act. The prominent SO₂-rich plumes discovered on Io, the water geysers on Enceladus, and nitrogen geysers on Triton are all spectacular examples. Cometary jets and outbursts may be further examples of gas-fluidized eruptions on the surfaces of small extra-terrestrial bodies.

Cinder cones. Cinder cones are steep-sided conical mounds of pumice and volcanic bombs that build up near the sources of more magma-rich volcanic flows. Driven by gas bubbling out of silica-poor magmas, these landforms often dot the traces of dikes feeding large flows, or stand in isolation over the sources of smaller flows. They may be built, destroyed, and rebuilt many times during any given eruption on Earth. They form because of the relatively small range to which pumice and volcanic bombs can be ejected from the vent and so pile up until landslides transport loose debris farther away from the vent. They are typically only a few kilometers across and 1 km high, with sides standing near the angle of repose for loose rock debris, around 30° from the horizontal. Cinder cones have been identified on Venus and Mars as well as Earth. On the Moon and other low-gravity bodies, the range of volcanic debris may be so large that cinder cones are much more spread out and thus do not achieve steep sides (McGetchin and Head, 1973). In this case cinder cones grade insensibly into pyroclastic deposits and the name cinder cone might not be appropriate.

Shield volcanoes. Silica-poor magmas, when they persistently erupt from a single center, produce low, broad volcanic mountains known as shield volcanoes. This name comes from the profile of an ancient Greek soldier's shield, placed concave-side down on a flat surface. The gases dissolved in silica-poor magmas readily escape near the vent and eruptions are characterized mainly by outpouring lava accompanied by only minor fire-fountaining. These eruptions are not explosive and mainly feed low-viscosity flows that carry liquid lava away from the vent. Shield volcanoes may spread hundreds of kilometers horizontally while achieving elevations of a few to a few tens of kilometers. The largest known example in the Solar System is Olympus Mons on Mars, with a basal diameter of 550 km and an elevation of 21 km above its base. Its summit is crowned by a complex caldera depression about 80 km across and 3 km deep. The slopes of shield volcanoes are low, much less than the angle of repose, and they are built up from many thousands of individual lava flows that either proceed from a summit caldera or are erupted from dikes breaching the flanks of the mound. The shield often contains a central magma chamber where rising magma accumulates before eruption. Eruption events that partially drain the magma chamber produce collapse calderas near the summit that alternately fill and reform during the life of the volcano. Shield volcanoes have been identified on Venus

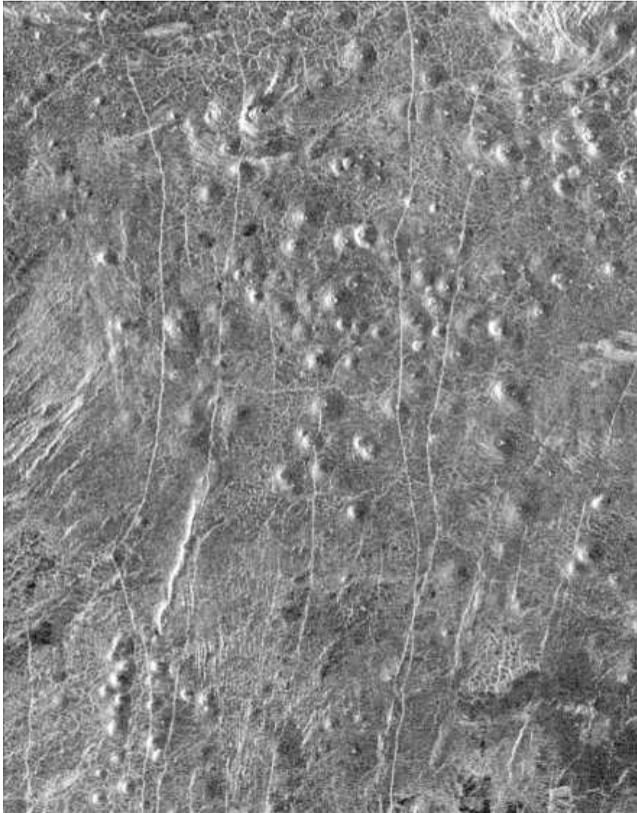


Figure 5.12 An extensive field of shield volcanoes on Venus. This field contains approximately 200 small volcanoes ranging from 2 to 12 km in diameter, many of which possess summit calderas. These are identified as shield volcanoes, although some cinder cones may occur among them. NASA Magellan image, left portion of PIA00465. Located at 110°E and 64° N. North is to the top.

(Figure 5.12), Earth (the Hawaiian volcanoes are the iconic examples), Mars, and perhaps on Mercury. Shield-like constructs also form the Moon's Aristarchus plateau and Io's Prometheus patera.

Long, fissure eruptions produce broad, nearly level volcanic plains that will be discussed in more detail in the next section. Near the fissure, exsolution of small quantities of gas may build cinder cones or, if less gas is present, small, typically elongated spatter ramparts around the dike where magma wells out of the ground.

Composite cones. Silica-rich magmas are highly viscous and volcanic material tends to build up around their eruptive centers because viscous flows are typically thick and short. As described above, their eruptions tend to be much more violent than silica-poor magmas because this type of magma is likely to be internally ruptured by bubble formation. Volcanic ash is created abundantly by such eruptions and pyroclastic flows spread

it far and wide, blanketing pre-existing terrain with smooth-surfaced deposits that may reach hundreds of meters in thickness. This type of magma is more likely than any other to form recognizable volcanic mountains. These constructs are often very steep-sided and are frequent sites of catastrophic rock avalanches that limit the size and extent of silica-rich volcanic mountains. Called “composite cones,” these piles of volcanic materials consist of alternating lava flows and volcanic ash deposits. All known examples occur on Earth and are the direct product of plate tectonics, their parent magmas being created by flux melting of silica-rich rocks in subduction zones, although it has recently been suggested that Ascræus Mons on Mars might be a composite cone.

Laccoliths. In addition to lavas that reach the surface, a few volcanic features are created by lava that is intruded beneath the surface. Horizontal sills may extend tens of kilometers from their source, but are difficult to recognize because they uplift the surface only a few meters to perhaps 100 m over a broad area. However, if the overburden above a sill is thin enough, it may become elastically unstable, flexing upward into a broad dome known as a laccolith. First recognized and named by G. K. Gilbert in the Henry Mountains of Utah (Gilbert, 1880), laccoliths have been found in many locations on Earth and the mechanics of their formation has been analyzed in detail (Johnson, 1970). Updoming results in characteristic radial fractures that may themselves be the source of surface lava flows. Laccoliths are typically a few kilometers to tens of kilometers in diameter. It has been suggested that several features on Mars are laccoliths, but definitive proof of a laccolithic structure is difficult on the basis of remote sensing alone.

Calderas. Calderas are one of the few negative-relief volcanic surface features. When large volumes of magma ascend over the same route from a persistent source, the liquid magma may accumulate beneath the surface at the level of neutral buoyancy and grow into a compact, long-lived, hot mass by displacing or partially assimilating the pre-existing cold rock. Called a magma chamber, slow cooling of the magma results in gradual crystallization and compositional changes. Rocks formed from large magma masses that slowly cool below the surface are called plutonic rocks and are characterized by large crystal sizes, typically millimeters to centimeters.

Eruptions may rapidly deplete the volume of liquid magma in a magma chamber. When this occurs the sudden loss of volume undermines the overlying rocks, which then collapse into the space formerly occupied by the magma, forming a depression. Such volcanic depressions are called calderas and their size reflects the diameter of the underlying magma chamber. Calderas on the terrestrial planets range from a few kilometers up to 100 km in diameter and range from a few 100 m in depth to many kilometers. They form at the sites of both silica-poor and silica-rich volcanic eruptions.

Not all volcanic centers display calderas: If the rate of magmatic replenishment to the chamber can keep up with the eruption rate, wholesale foundering of the surface into the magma chamber does not occur and a caldera never forms. Nevertheless, erupted magma piles up on the surface and a large volcanic edifice may be constructed from the products of many small eruptive events.

5.3 Lava flows, domes, and plateaus

Lava flows form when predominantly liquid magma reaches the surface and flows away from the vent or fissure, eventually to cool into a solid surface deposit. Magmas are not simple liquids: They almost universally contain bubbles formed by exsolved volatiles and crystals created during cooling before eruption. Rapidly erupted magmas may also be loaded with solid xenoliths, inclusions of rock from either a deep source region or the walls of the rock surrounding the magma's route of ascent. For this reason they exhibit complex rheologies, which are reflected by their deposits.

5.3.1 Lava flow morphology

Magma that erupts onto a planetary surface is called lava. When this hot, complex liquid flows out onto the surface of a planet it suddenly enters a much cooler environment. The response of the lava's surface to this rapid cooling creates a variety of textures that depend strongly on the magma composition and cooling rate. The interior of the flow cools more slowly and behaves very differently from the lava at its surface.

Highly viscous, silica-rich lavas form short, stubby flows that usually contain a large proportion of glass upon cooling. Differential thermal stresses fracture the surface of the hot magma into glassy fragments that bury and then insulate the interior of the flow. Slow, viscous flows usually exhibit a wavy, strongly textured surface on the scale of tens to hundreds of meters that is later cut by deep cooling cracks.

Pillow lava. More fluid lavas develop surface textures that are described as being of four general types. Submarine flows cool very quickly upon contact with water. The glassy surface is splintered into fine glassy fragments (called palagonite), while the mass of the magma collects into lava-filled sacks that often detach from the flow front and pile up in front of it, forming structures known as pillows. Individual pillows range from a few tens of centimeters to meters in diameter and their presence in a cooled lava flow is diagnostic of an underwater eruption. Subaerial flows cool more slowly and produce surface textures denoted pahoehoe, aa, or block types.

The peculiar surface textures of silica-based lavas derive in part from the tendency of silica tetrahedra to polymerize. At high temperatures (between about 800°C and 1070°C) highly polymerized silica glass behaves like rubber (a high-polymer substance based on carbon). Capable of sustaining large strains without breaking, the rubbery surface of cooling silicate lavas can inflate with liquid lava like a balloon or, under compression, collapse into folds resembling drapery on a scale of tens of centimeters. Incautious Hawaiian volcanologists once impressed onlookers by jumping up and down on fresh lava flows, which responded like a giant waterbed (this practice is now forbidden due to several unfortunate accidents).

Aa lava. Subaerial lava that is depleted of volatiles or moving rapidly develops a clinkery, fractal surface known by the Hawaiian name aa. Its surface disaggregates into porous, decimeter-sized fragments as the flow moves. Glassy spines pull out of the hot, separating fragments like the sugar-rich spines of pulled taffy. Aa surfaces are almost impossible to

walk across and tend to shred shoes or boots. The fronts of aa flows are typically a few to tens of meters high and advance like a caterpillar tractor tread, with cooled chunks of aa falling from the top of the steep-fronted flow as hot lava in its interior overruns the previously fallen debris. A section of a cooled aa flow, thus, shows both a clinkery basal zone and a rubbly top, separated by a more massive zone of vesicular lava. Although the surfaces of aa flows are unforgettable for those who have experienced them, they are not voluminous on the Earth's surface.

Block lava. Block lavas, as their name suggests, are composed of meter-scale polyhedral blocks of lava. Formed from more viscous lava than either aa or pahoehoe, on Earth they form thick, short flows and seem to advance in a mode similar to aa. They are also not very voluminous on Earth.

Pahoehoe lava. Pahoehoe is, by far, the most abundant type of lava on Earth and probably on the other terrestrial planets. It forms both small flows and the giant sheets that blanket Earth's most extensive flood basalt provinces. Its name is derived from a Hawaiian word that indicates "smooth going." The surface of fresh pahoehoe is smooth, with a thin glassy rind that weathers rapidly on Earth. Its surface is marked by broad billows and swales and is locally puckered into drapery-like folds. Pahoehoe advances by a unique mechanism that has only recently been understood. Called "inflation," this mode of motion permits it to travel large distances with only modest eruption rates (Self *et al.*, 1998). Inflation was discovered during observations of active pahoehoe lava flows in Hawaii (Hon *et al.*, 1994). Flows first advance as a thin sheet that rapidly covers the terrain. The upper surface of the sheet cools rapidly, forming an insulating blanket under which hot lava continues to flow. On a timescale of hours, hot, fluid lava intrudes beneath the chilled surface, uplifting it and creating a nearly planar surface. Deep cracks form near the margins of inflated flows as the upper surface is lifted above the original base and slabs of chilled crust tilt away from the main mass of the flow. Uninflated areas form irregular depressions in the overall, nearly uniform, lava surface. Individual pahoehoe flows achieve thicknesses of tens of meters in flood basalt provinces and may continue to inflate and spread for more than a year. Over time, the lava feeding an inflated flow organizes into distinct streams, or "tubes," beneath the thickening crust. The flow velocity in an individual tube thus exceeds the rate of advance of the lava flow as a whole. When the supply of fresh lava from the vent declines, these tubes may drain and remain open as lava caves, or in the case of a thinner cover, the empty lava tubes may collapse to leave sinuous channels on the flow surface. The surface of large pahoehoe flows is locally marked by pits where inflation failed to occur, mounds called "tumuli" where lava locally broke through the surface when lava channels became blocked and small mounds accumulated, and "rootless cones" where the lava flowed over wet ground, creating small phreatic explosions that threw up blocky mounds (often called "hornitos") or larger rimmed craters up to a few hundred meters in diameter.

Columnar jointing. As lava flows cool and crystallize the lava shrinks and cracks open throughout the solidified flow. Because lava flows cool from outside inward, cracks initiate on their surfaces and propagate toward their interiors. Uniform contraction of a thin surface layer typically produces a polygonal fracture pattern, familiar from the surface of drying mud

puddles. As cooling cracks propagate into the flow perpendicular to the cooling surface, they elongate, creating a pattern of polygonal columns called “columnar jointing.” Columnar joints are often prominent at the eroded edges of lava flows, forming spectacular outcrops at Devils Postpile in California and the Giant’s Causeway in Ireland. Columnar joints form in both silica-poor and silica-rich lava flows as well as pyroclastic deposits. Columns are typically tens of centimeters to meters in width. They have recently been observed on Mars, in lava flows outcropping on the rims of the great canyons. The formation of columnar joints is a universal process that occurs for any cooling, shrinking mass and can be analyzed in terms of fundamental principles (Goehring *et al.*, 2009).

5.3.2 The mechanics of lava flows

Spurred by the hazards posed by advancing lava flows, volcanologists have made many efforts to compute the length and width of lava flows from their basic properties. Planetary scientists, observing lava flows on other planets, have inverted these efforts to compute the properties of lava from the morphology of the final flow. Although early efforts treated lava as a Newtonian fluid, it is now agreed that lava behaves as a Bingham fluid and modern flow models are based on this rheology. The Bingham model provides a number of simple relations for the dimensions of a lava flow (Moore *et al.*, 1978). One of the goals of planetary volcanology is to relate estimates of the physical properties of the lava to its composition and, thus, learn about the chemistry of planetary crusts and mantles without having to directly sample them.

The thickness H of an extensive sheet of lava resting on a uniform slope standing at angle α to the horizontal is given in terms of the Bingham yield stress as simply:

$$H = \frac{Y_B}{\rho g \sin \alpha} \quad (5.10)$$

where g is the acceleration of gravity and ρ is the density of the lava. This formula strictly applies only to an infinitely wide sheet of lava and is derived by setting the shear stress at the base of the lava flow equal to the Bingham yield stress (Figure 5.13a). If the thickness and other parameters of a lava flow can be estimated, this equation can be inverted to determine the Bingham yield stress. This model makes the uncomfortable prediction that a lava flow on a level surface ($\alpha = 0$) is infinitely thick. A more sophisticated model, still applying the Bingham rheology, examines the force equilibrium of a lava sheet of variable thickness resting on a level surface (Figure 5.13b). If $y(x)$ is the thickness of the lava flow and x is the distance to the edge of the flow, by balancing the horizontal thrust of the lava toward its edge at x , given by $\frac{1}{2} \rho g y(x)^2$, by the basal force at the yield stress, xY_B , for a thin slice of the flow, an equation for the thickness of the lava flow at any distance from its edge is found:

$$y(x) = \sqrt{\frac{2xY_B}{\rho g}}. \quad (5.11)$$

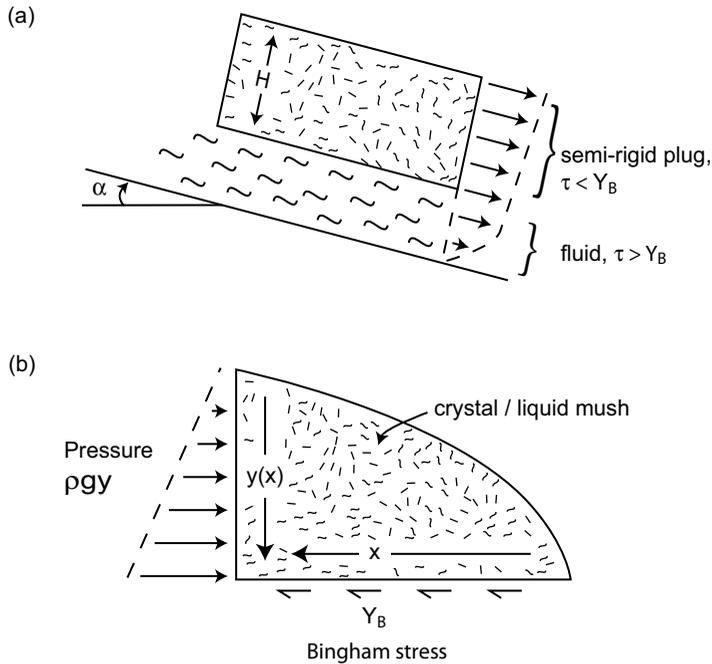


Figure 5.13 Panel (a) shows the shear stress acting on the base of an infinitely wide sheet of lava resting on a surface sloping at a uniform angle α . The shear stress acting on its base is $\rho g H \sin \alpha$. The Bingham rheology implies that, so long as the shear stress is less than the Bingham yield stress Y_B , the lava does not deform. At the higher shear stresses found beneath the uppermost semi-rigid plug, the lava flows like a viscous fluid. Panel (b) shows the stresses near the edge of a lava flow, where the horizontal thrust of the pressure in the lava flow to the left is balanced against the shear resistance of the Bingham material to the right. The profile of the lava flow margin is a parabola, as described in the text.

This is the equation of a parabola and, indeed, measurements of the shape of the edges of many lava flows give approximately parabolic profiles from which the Bingham yield stress can be computed. This equation is often applied to estimate the Bingham yield stress from the width of a lava flow. So long as the cross-profile of the flow is crudely parabolic (not flat-topped: If the flow has a flat top, this indicates that the lava flow thickness is controlled by the slope, through Equation (5.10)), then the width of the flow $W = 2x$ and its centerline thickness H determines the Bingham yield stress:

$$Y_B = \frac{\rho g H^2}{W}. \quad (5.12)$$

Bingham yield stress. Equation (5.11) makes the prediction that the thickness of a lava flow on a level surface increases as its width increases. This might be a sensible prediction, but planetary surfaces are seldom level over very long distances. A better model results from combining Equations (5.10) and (5.11) to model the edge of a wide lava flow on a

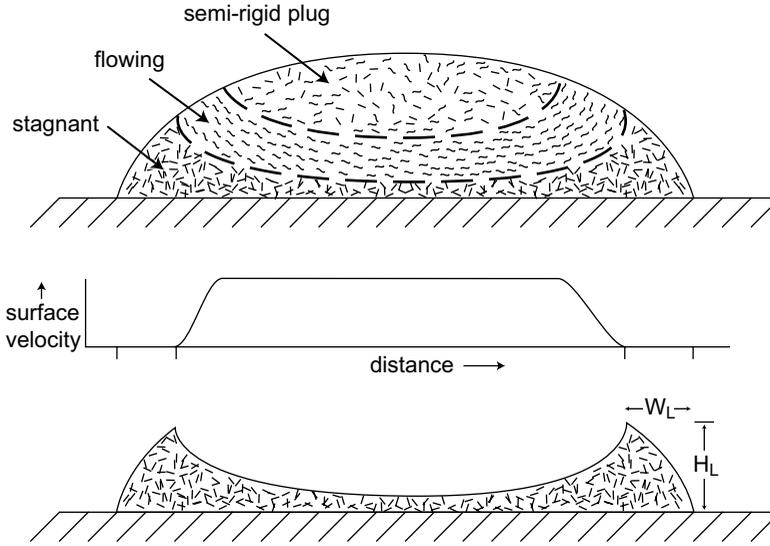


Figure 5.14 Cross section of a lava flow and the leveed channel it leaves behind. The upper section shows the profile of the lava flow at its most active. The chilled bottom is frozen to the bed, but the hotter lava above it flows as a viscous fluid so long as the shear stress exceeds the Bingham yield stress. In low-stress regions the material moves as a semi-rigid plug, similar to the infinite flow in Figure 5.13a. The surface velocity of the flow is shown in the middle panel. The lower section shows the levees that remain after the lava drains away. The width and height of the levees can be related to the Bingham yield stress.

gently sloping surface. In this case, the thickness of the center of a wide lava flow is given by Equation (5.10) while its edges are described by (5.11). The combined equations also give a nice description of the formation of the levees sometimes observed flanking lava flows. So long as lava is erupting at a high rate, the profile of the lava flow bulges up in the middle. However, as the eruption rate declines, the lava runs out of the channel, leaving the material in the cooler levees behind (see Figure 5.14). The levee width W_L and height H_L are easily measured on images of the flow so, applying Equation (5.11), the Bingham yield stress can be computed from these observables:

$$Y_B = \frac{\rho g H_L^2}{2 W_L}. \quad (5.13)$$

An alternative formula can be derived by combining this equation with (5.10) to eliminate the flow thickness H_L :

$$Y_B = 2 \rho g W_L \sin^2 \alpha. \quad (5.14)$$

The Bingham yield stress measured in this way suffers from the problem that the yield stress applies to the stagnant levees, not the hotter active portion of the flow, but it does give an order-of-magnitude estimate useful for comparisons between lava flows.

Lava viscosity. Once the Bingham yield stress is exceeded, a Bingham material flows as a Newtonian viscous fluid. The Newtonian rheology has also been widely used to estimate the viscosity η of actively flowing lava by measuring the surface velocity U_{surf} and estimating the flow depth H . In the case of laminar flow, the velocity profile is parabolic and the surface velocity is:

$$U_{\text{surf}} = \frac{\rho g H^2 \sin \alpha}{2 \eta}. \quad (5.15)$$

This velocity is approximately related to the total lava discharge Q_E (volume/unit time) of the channel of width W_c by:

$$Q_E = \frac{2}{3} U_{\text{surf}} H W_c. \quad (5.16)$$

Similar equations can be derived for turbulent flow, but because most known lava flows seem to have moved in the laminar regime, with low Reynolds number, they are not tabulated here.

Equations (5.15) and (5.16) are the basis of a widely used viscosity estimate (Nichols, 1939) called the Jeffreys' equation (after a 1925 paper by Harold Jeffreys):

$$\eta = \frac{\rho g H^3 W_c \sin \alpha}{n Q_E} \quad (5.17)$$

where n is a numerical parameter equal to 3 for broad flows and 4 for narrow flows. This equation assumes that lava is a Newtonian fluid and so its predictions for planetary lava flows are open to question.

For a Bingham fluid, the flow depth H should properly be the depth of the fluid excluding the semi-rigid plug of lava on top of the flow (the flowing portion must be subject to a shear stress exceeding the Bingham yield stress, and so requires some overburden before this stress is reached) and the overall discharge should include the volume of this plug. In practice these distinctions are usually ignored, as there is no simple way of separating them from image data. Thus, planetary estimates of the viscosity and Bingham yield stress are only rough estimates, not precise measurements.

Lava effusion rate. The effusion rate of lava from a feeder vent provides information about how magma is transported beneath the surface of a planet and is, thus, important for comparing volcanism on different bodies. It also plays a role in determining the maximum length of a lava flow. The total volume V_L of a lava flow can be estimated from its area A and thickness H : $V_L = A H$. If the duration of the eruption t_e is known, then the average effusion rate is simply $Q_E = V_L / t_e = AH/t_e$. However, the duration of past eruptions cannot be measured directly and so other ways of estimating eruption rates must be found. One current approach is to use a dimensionless measure of heat transport, the Grätz number, G_z , which is the ratio between the heat advected in a flow to the heat conducted. The Grätz number for a lava flow is defined as:

$$G_z = \frac{Q_E H}{\kappa A} \quad (5.18)$$

where κ is the thermal diffusivity of the lava composing the flow. It has been observed that this number is typically about 300 for basaltic lava flowing in channels (Gregg and Fink, 1999). Using this number, Equation (5.18) can readily be inverted to determine the effusion rate. However, tube-fed pahoehoe flows probably cool much more slowly and this may greatly overestimate the effusion rate for such flows. Unfortunately, no systematic estimates yet exist for the Grätz number of pahoehoe flows, although one estimate of the cooling time of the crust (Hon *et al.*, 1994) suggests that it may be of order 10. Another estimate from the 1300 km² Roza flow of the Columbia River Basalt Province gives $G_z \sim 32$. Eruption rates for inflated flows based on the Grätz number for channel flows may thus be about 10 times too large.

An estimate of the effusion rate for a single lava flow on a surface of average slope α and Bingham yield stress Y_B can be obtained by combining Equations (5.10) and (5.18):

$$Q_E = \frac{\kappa A G_z}{Y_B} \rho g \sin \alpha. \quad (5.19)$$

Equations of this sort can be used to make models of lava flow formation if the material parameters of the flow can be estimated. Rearrangement of this equation indicates that the effusion rate is probably the major factor in controlling the final area of a lava flow. Table 5.6 collects a number of estimates of the parameters describing lava flows on the terrestrial planets and moons.

Lava composition and rheology. It is widely believed that the Bingham yield stress is correlated with silica content, as is the viscosity. Data compilations suggest that yield stresses in the range of 100 Pa indicate basalt with silica contents of about 40 wt%, whereas values near 10⁵ Pa indicate andesitic lavas with silica contents around 65 wt%. However, this relationship does not seem to be monotonic at higher silica contents, as rhyolites also have yield stresses in the range of 10⁵ Pa (Moore *et al.*, 1978). It is clear from Table 5.6 that the properties of silicate lavas are generally similar on all of the terrestrial planets. Silica-rich lavas tend to have higher Bingham strengths and viscosities than silica-poor lavas. The major exception is Io, where very high eruption temperatures produce weak, highly fluid lavas. Eruption rates are highly variable and it seems that the eruption rate, more than any other factor, is the primary determinant of the size of an individual lava flow.

5.3.3 Lava domes, channels, and plateaus

Lava flows are highly complex landforms whose surface features are too varied to treat in a chapter of this length, so the interested reader who wants to go further is urged to consult some of the specialized works listed at the end of this chapter. However, a few features that are prominent in images of planetary surfaces deserve a brief mention here.

Table 5.6 *Rheologic properties of lava flows in the Solar System*

Location (type)	Bingham yield strength (Pa)	Viscosity (Pa-s)	Effusion rate (m ³ /s)
Earth			
Mauna Loa, HI (basalt)	$(3.5-72) \times 10^2$	$1.4 \times 10^2 - 5.6 \times 10^6$	417-556
Makaopuhi, HI (basalt)	$(8-70) \times 10^3$	$(7-45) \times 10^2$	–
Mount Etna, Italy (basalt)	9.4×10^3	9.4×10^3	0.3-0.5
Sabancaya, Peru (andesite)	$5 \times 10^4 - 1.6 \times 10^6$	$7.3 \times 10^9 - 1.6 \times 10^{13}$	1-13
Mono Craters, CA (rhyolite)	$(1.2-3) \times 10^5$	–	–
Moon			
Mare Imbrium	$(1.5-4.2) \times 10^2$	–	–
Gruithuisen domes	$(7.7-14) \times 10^4$	$(3.2-14) \times 10^8$	5.5-120
Venus			
Artemis festoons	$(4.1-13) \times 10^4$	$7 \times 10^6 - 7.3 \times 10^9$	$(2.5-10) \times 10^3$
Atalanta Festoon	1.2×10^5	2.3×10^9	950
Mars			
Arsia Mons	$(2.5-3.9) \times 10^3$	9.7×10^5	$(5.6-43) \times 10^3$
Ascraeus Mons	$(3.3-83) \times 10^3$	$(2.1-640) \times 10^3$	18-60
Tharsis plains ^a	$(1.2-2.4) \times 10^2$	$(8-58) \times 10^2$	$(2-25) \times 10^2$
Io			
Shield volcanoes ^b	$(1-10) \times 10^1$	10^3-10^5	~3000
Ariel cryovolcanism Flows ^c	$(6.7-37) \times 10^3$	$(9-45) \times 10^{14}$	–

Data from Hiesinger *et al.* (2007), except:

^a Hauber *et al.* (2010)

^b Schenk *et al.* (2004)

^c Melosh and Janes (1989)

Pancake domes. Figure 5.15 illustrates a cluster of “pancake domes” on Venus. These domes resemble silica-rich rhyolite domes on the Earth (an example is the Mono Craters in California), although the 25 km-wide Venusian domes are larger than most terrestrial occurrences. These constructs are believed to form from the extrusion of highly viscous lava that flows only a short distance from an underlying vent. When lava of this type erupts onto steep slopes the lava oozes downhill to freeze into thick, stubby, elongated lobes.

Sinuuous rilles. First named by German astronomer Johann Schröter (1745–1816) in 1787, sinuous rilles immediately caught the attention of some of the first observers of the Moon, who thought that they had discovered river valleys. They often head in circular to irregular pits and tend to decrease in width as they meander downslope in wide curves (Figure 5.16). Typically several kilometers wide and hundreds of meters deep, they may

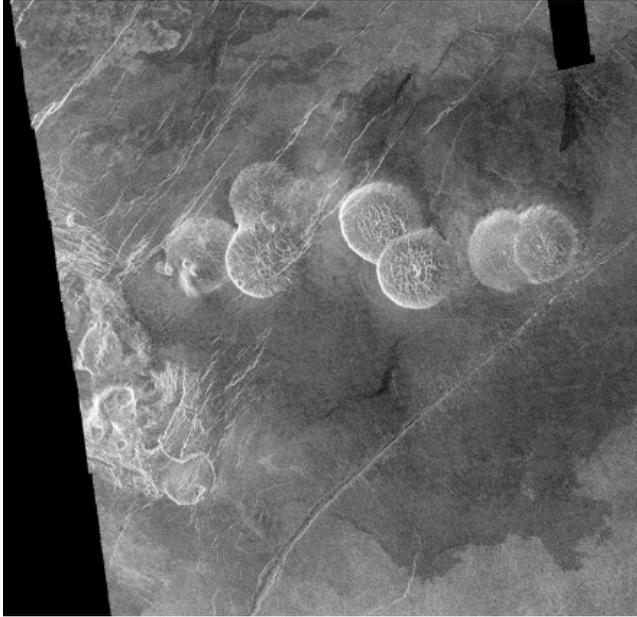


Figure 5.15 Pancake domes on Venus. These seven domes in eastern Alpha Regio are each about 25 km in diameter and 750 m high. They are interpreted as extrusions of very viscous lava from a central source. NASA Magellan radar image PIA00215. North is up.

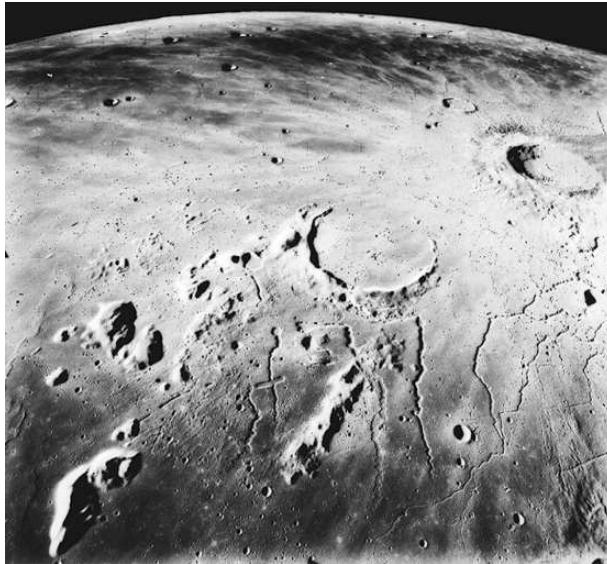


Figure 5.16 Apollo 15 image of the Aristarchus plateau of the Moon, showing flooded craters and sinuous rilles of this highly volcanic region. The flooded crater in the foreground is Prinz, 46 km in diameter. Aristarchus crater, 40 km diameter, is in the right background. NASA image A15_m_2606.

stretch hundreds of kilometers in length. Some appear to stop for a short distance and then begin again as if whatever flowed through them went underground for a while. Sinuous rilles occasionally degenerate downslope into a line of rimless pit craters, again suggesting collapse into an underlying cavity. A small rille on the floor of the much larger Schröter's Rille seems to wind enigmatically in and out of its side walls. They are invariably associated with lava plains. The Apollo 15 astronauts famously landed on the margin of Hadley Rille, but were unable to demonstrate its origin other than to show that the rocks outcropping on its rim are basalts.

Sinuuous rilles are observed on the Earth, Mars, and Venus as well as the Moon. All of these characteristics suggest that sinuous rilles represent channels through which lava once flowed. However, much controversy still centers about how completely they were filled, when they were active, and whether they are collapsed lava tubes or were once open to the sky. Some of them cut deep into the surrounding surface, suggesting that the flowing lava somehow deepened its channel. Much discussion has focused on the process of thermal erosion, by which the hot, flowing lava heats and softens the underlying rocks, melting them away and, thus, slowly deepening the channel. On the other hand, flowing lava is quite capable of quarrying away jointed blocks in its bed through the hydrodynamic "plucking" process by which water carves channels into bedrock. While thermal erosion is theoretically capable of deepening channels, its action has never been unambiguously demonstrated on the Earth, whereas there are good Hawaiian examples of plucking.

Lava plateaus. Lava plateaus are stacks of many individual lava flows. When a rising, hot, mantle plume arrives near a planet's surface it may deliver both heat and differentiated melts to the base of the crust for a long period of time. In this case magma spills out onto the surface in many, perhaps hundreds to thousands, of individual flows. So long as magma can continue to penetrate the lava flows already congealed on the surface, more material builds up, creating a thick pile of individual flows with a combined volume that may rival the volume of the crust itself.

On the Moon, lava began to erupt through the thin nearside crust about 500 Myr after the large basins were themselves created by impacts. Because of the long time interval between basin formation and the lava flows, there does not seem to be any genetic connection: The impacts did not initiate the volcanism. Instead, the impacts created topographically low basins and thin crust through which the lava extruded. Although individual lunar flows are hundreds of meters thick, owing to the low lunar gravity, it required the accumulation of many individual flows to build up the multi-kilometer thick piles of lava that we now recognize as the lunar mare.

Similar stacks of individual lava flows from long-continued volcanism created the tens of kilometers thick Tharsis plateau on Mars. Thinner lava plains cover much of the rest of the surface of Mars, with individual thin flows extending thousands of kilometers. Most of the surface of Venus was covered by extensive lava flows around 700 Myr ago, obliterating most of whatever surface Venus originally possessed. A single lava channel, Baltis Vallis, on Venus stretches 6800 kilometers across its surface. The Earth possesses dozens of broad, large igneous provinces that have erupted hundreds of thousands of cubic kilometers of

basalt throughout the geologic history of our planet, each eruptive episode lasting only a few million years. Recent images returned from the MESSENGER spacecraft show that Mercury's extensive intercrater plains are volcanic, again indicating the importance of repeated volcanic eruptions.

Io is the volcanic body *par excellence*, whose crust seems to be entirely created by repeated volcanic flows, which renew its surface at the average rate of 1.5 cm/yr. Although its visible surface is largely coated with volatile sulfur and SO₂, its overall density and the high temperatures of its lavas measured by the Galileo probe indicate that its volcanism is predominantly silicic, perhaps dominated by ultramafic lavas.

Less is known of the water-mediated cryovolcanism on the icy satellites, but it is clear that flowing liquids have covered many of the icy satellites' surfaces. Volcanism has been active on nearly all of the solid bodies in the Solar System, so understanding this process is a vital part of the study of planetary surfaces in general.

Further reading

The history of investigation of volcanoes and magma on the Earth is engagingly told in the history by Sigurdsson (1999). The book by Williams and McBirney (1979) provides excellent quantitative coverage of the basic ideas of volcanic phenomena, but is now becoming somewhat dated. A more up-to-date reference with similar coverage is Schmincke (2003), but the best and most readable reference, although not as quantitative as Williams and McBirney is Francis and Oppenheimer (2003). A good general reference to the chemistry of rocks and melting, as well as much more, is McSween *et al.* (2003). Io is the volcanic moon *par excellence* and an entire book is now devoted to it Davies (2007).

Exercises

Note: As for all problems of this kind, your best guide to a correct answer is to make sure that the dimensional units of all results are correct!

5.1 Squeezing magma sponges

Derive Equation (5.6) for the timescale over which magma percolates out of a magma-saturated layer of thickness h by equating the volume discharge per unit area Q times the percolation time $t_{\text{percolate}}$ to the volume of melt ϕh in the layer.

Use this equation to estimate the timescale over which the 100 km thick asthenosphere underlying oceanic plates on Earth would lose 10% of its melt if the grain size in the mantle is about 1 mm and the viscosity of hot basaltic melt is 10⁴ Pa-s.

Now shift to the outer Solar System and *estimate* the rate at which water "magma" segregated from the body of Uranus' 1160 km diameter satellite Ariel (Voyager imaged lava flows on its surface). Ariel's mean density is 1660 kg/m³ and the viscosity of water at its

melting point is about 1.5×10^{-3} Pa-s. What does this tell you about the ability of planets to retain melt in their interiors?

5.2 Feeding Ariel's volcanoes

If pure liquid water ascends from the interior of Ariel by means of dikes of width about 1 cm, use Equation (5.8) to estimate the mean velocity of the water in the dike. Next, use Equation (5.7) to estimate the vertical depth L_c of the dike as it rises toward the surface. Finally, assuming that the horizontal extent of a dike segment is approximately the same as its vertical depth, compute the volume of water carried by this dike. Combining the mean velocity and area of the dike as it breaches the surface, estimate the eruption rate of water onto the surface. At this rate, how long would it take to build up a cryovolcano 10 km in diameter and 1 km high? How many dikes must discharge their contents to build the volcano?

5.3 Plumbing Enceladus' geysers

The NASA–ESA Cassini Mission discovered that water-dominated geysers erupt continuously from the south pole of Enceladus, a Saturnian satellite about 500 km in diameter. The geysers spew out of four long fissures called “tiger stripes” whose hottest portions extend about 50 km horizontally. The CISR Infrared Spectrometer observed an excess heat flow from the entire region of about 6 GW. If the liquid water freezes and cools to the ambient temperature of 69 K, use Equation (5.1) to estimate the volume eruption rate, per unit length of the fissures, of water necessary to supply this heat flux. Supposing that the geysers are fed by pure liquid water, apply Equation (5.8) (plus a little creative thinking) to estimate the width of the dikes feeding water to the surface and the mean velocity of the water moving up the dike. Finally, use either Equation (5.7) or (5.9) to estimate the depth of the fissures feeding the eruption. If these eruptions are fed by “quanta” of water trapped in rising dikes of these dimensions, what is the duration of a single eruptive pulse as an individual dike breaches the surface? Note that there are multiple valid ways to get the correct answer.

Useful data: The latent heat of freezing for water is 334 kJ/kg and its heat capacity is 4.2 kJ/kg-K. The viscosity of water is about 1.5×10^{-3} Pa-s. Young's modulus of Enceladus' ice crust is about 10^{10} Pa. The density contrast between the erupting fluid and the surrounding ice is almost completely unknown. A crude estimate is to suppose that it is about 10% of the density of ice. The surface acceleration of gravity on Enceladus is 0.11 m/s^2 .

5.4 Volcanic bombs in orbit: a natural answer to StarWars

Ronnie, an inquisitive sixth-grade visitor to the planetarium, wants to know if big, noisy volcanoes on Earth can eject rocks into space. Johnnie, another budding intellect, thinks that lunar volcanoes eject tektites. Use your knowledge of the thermodynamics of expansion to compute the *maximum* expansion velocity $v_\infty = \sqrt{2h}$, where h is the specific enthalpy of

the expanding gas for the volcanic gases CO , H_2O , and H_2 , at a typical eruption temperature of 1200°C . Compare these velocities to the escape velocities of the Earth, Mars, and the Moon.

If water vapor is the primary volcanic gas on Mars, how high an eruption temperature would be required for Martian volcanoes to eject volcanic bombs from the planet? How hot a volcano is needed for it to eject material from Earth? Do you think that Ronnie's and Johnnie's ideas make any sense?

Useful data: The specific enthalpy h of a gas is approximately $h = c_p T$, where T is the absolute temperature and c_p is the specific heat at constant pressure, $c_p = 7/2 R$, where R is the gas constant, $8.317 \text{ J/mol}\cdot\text{K}$.

5.5 Go with the flow

- Steep flow fronts are observed at the edges of broad, extensive lava flows on the lunar Mare. These lava flows are considerably thicker than terrestrial lava flows, often reaching 100 m in height. The average slope of one such flow is about 0.5° . Use Equation (5.10) to compute the Bingham yield stress of this lava flow and compare it to terrestrial lava flows. Is lunar magma substantially stronger than terrestrial magma?
- Viking images of Olympus Mons on Mars reveal numerous leveed lava flows running down its flanks, which slope at about 7° to the horizontal. The widths of the levees are easily measured from orbit. One large flow is observed to possess levees about 1 km wide. Estimate the Bingham yield stress of this flow and compare it to that measured on terrestrial lava flows. What can you deduce (if anything) about the magma that created this flow? This leveed channel is observed to have fed a small lava flow on the flanks of Olympus Mons that expanded to about 8 km wide and ran 50 km down the slope. Estimate the effusion rate of this flow. What additional information would you need to estimate the viscosity of the lava? Can you envisage obtaining this information from orbit?

5.6 Big volcanoes on little planets

Use the theory of lava flow lengths derived in Section 5.3.2 to relate the radius of a volcanic edifice, L , with a height H to the eruption rate Q_E . Assume that central eruptions last long enough that the length of each flow that builds up the edifice is limited by its solidification time. That is, if L is of order $Q_E t_e / h$, where t_e is the duration of the flow and h is its thickness, then t_e is of order h^2 / κ , where the thermal diffusivity of rock, κ , is about $10^{-6} \text{ m}^2/\text{s}$. Assume that the thickness of the flow is given by the Bingham yield stress Y_B ,

$$h = Y_B / (\rho g \sin \alpha)$$

where α is the mean angle of the volcano's slope, $\tan \alpha = H/L$. Derive an expression relating volcano radius (that is, maximum lava flow length, L) to eruption rate Q_E and

height H . Note that you will have to make some approximations to account for the fact that the volcano is circular in plan while the estimates above for L and h are on a per unit width basis.

Use this relation to derive an eruption rate and mean flow thickness for Olympus Mons on Mars, a 400 km diameter central volcano made predominantly of basaltic lava, where $Y_B = 10^3$ Pa. The average surface slope of this 24 km high volcanic edifice is about 7° . Compare the derived eruption rate to the typical eruption rate of terrestrial basaltic volcanoes, ca. 3×10^7 m³/day. What does this mean?

Note: There is no single “right answer” to this problem, which requires you to make a number of “reasonable” approximations. This problem is a thinking exercise in how simple theories are concocted.